New fossils of small and medium-sized bovids from the Early Pleistocene Site of Shanshenmiaozui in Nihewan Basin, North China

TONG Hao-Wen[1,2,3*] ZHANG Bei[4] CHEN Xi[5] WANG Xiao-Min[6]

(1 *Key Laboratory of Vertebrate Evolution and Human Origins of Chinese Academy of Sciences*, *Institute of Vertebrate Paleontology and Paleoanthropology*, *Chinese Academy of Sciences* Beijing 100044
* Corresponding author: tonghaowen@ivpp.ac.cn)
(2 *CAS Center for Excellence in Life and Paleoenvironment* Beijing 100044)
(3 *University of Chinese Academy of Sciences* Beijing 100049)
(4 *Beijing Museum of Natural History* Beijing 100050)
(5 *Nanjing Normal University* Nanjing 210023)
(6 *Institute of Archaeology*, *Chinese Academy of Social Sciences* Beijing 100710)

Abstract Shanshenmiaozui site in Nihewan Basin in North China is a recently discovered Early Pleistocene site which yields rich and diverse mammalian fossils. In the fauna, the small and medium-sized bovid fossils are well represented and can be referred to the following taxa: *Spirocerus wongi*, *Gazella sinensis*, *Ovis shantungensis* and *Megalovis piveteaui* respectively, among which *G. sinensis* is the dominate species. *S. wongi* and *G. sinensis* are mainly represented by horn-cores and partial skull bones as well as mandibles; in addition, metacarpal and/or metatarsal bones were also recognized for all of the four species. The horn-cores are easy to be identified to the species level, while the dentitions and the postcranial bones underwent a series of examinations and comparisons before getting properly determined and referred to the most approximate taxa. Among the postcranial bones, the metapodials, especially to the metacarpal bones special attentions were paid, which are crucial not only for taxonomic identification, but also for phylogenetic and paleoecological reconstructions; the previously misidentified metapodial specimens in Nihewan fauna were reconsidered in this paper. In the SSMZ fauna, the bovid guild is dominated by *Gazella* and *Bison*, which indicates steppe was the most important biome in Nihewan Basin during Early Pleistocene.

Key words Shanshenmiaozui, Nihewan, China; Early Pleistocene; small-medium bovid; new fossils

Citation Tong H W, Zhang B, Chen X et al., in press. New fossils of small and medium-sized bovids from the Early Pleistocene Site of Shanshenmiaozui in Nihewan Basin, North China. Vertebrata PalAsiatica.

国家自然科学基金(批准号：42172021, 41572003)、中国科学院战略性先导科技专项(B类) (编号：XDB26000000)和国家重点研发计划(编号：2020YFC1521500)资助。
收稿日期：2021-09-13

1 Introduction

Nihewan (=Nihowan which is abbreviated as “NIH” in the MNHN collections) Basin is located at Yangyuan County of Hebei Province in North China, which is famous for its late Cenozoic fluvio-lacustrine deposit sequence and the Early Pleistocene mammalian fauna—the Nihewan Fauna. Nihewan fauna was discovered in the 1920s and published in 1930 by Teilhard de Chardin and Piveteau. The early excavations were conducted mainly in the areas around the Xiashagou and Nihewan villages on the north bank of the Sanggan River (Sangkanho).

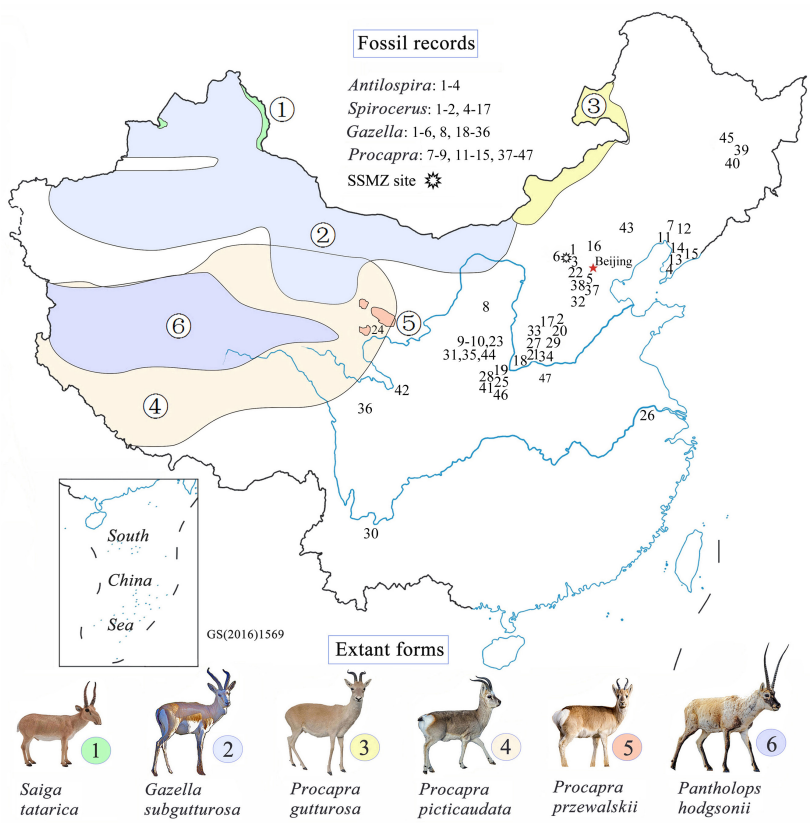

Fig. 1 Location of Shanshenmiaozui (SSMZ) site, with distributional map of living antelopes and related fossil forms of the Pleistocene Epoch in China

Data for the extant taxa are from Jiang (2004), Smith and Xie (2008). Fossil localities: 1. Xiashagou of Nihewan; 2. Yushe; 3. Dongdoubi of Yuxian; 4. Jinyuan Cave; 5. Zhoukoudian Loc.1; 6. Xujiayao; 7. Mashandong; 8. Salawusu; 9. Xifeng of Qingyang; 10. Loufangzi; 11. Jinniushan; 12. Miaohoushan; 13. Haimao of Dalian; 14. Gulongshan; 15. Xiaogushan; 16. Chicheng; 17. Dingcun; 18. Xihoudu; 19. Tianshuigou of Dali; 20. Wenxi; 21. Pinglu; 22. Danangou of Yuxian; 23. Bajiazui; 24. Gonghe; 25. Yangguo; 26. Tuozidong; 27. Tunliu; 28. Banpo; 29. Linyi; 30. Yuanmou; 31. Heshui; 32. Xingtai; 33. Xiaochangcun; 34. Wuwang of Linyi; 35. Gengjiagou; 36. Luhuo; 37. Zhoukoudian Loc.15; 38. Upper Cave; 39. Guxiangtun; 40. Zhoujiayoufang; 41. Dali Man site; 42. Aba; 43. Chifeng; 44. Rouyuan; 45. Yanjiagang; 46. Yuhongcun of Dali; 47. Lingjing

In the past decades, much more explorations and excavations have been conducted, and almost all of them were took place on the southern bank of the Sanggan River, and the Shanshenmiaozui Site (Fig. 1) is among the most productive sites in mammalian fossils. Up to now, 25 species, including undetermined species, have been recognized and/or published: *Allactaga sibirica* (Tong et al., 2021), *Ochotonoides complicidens* (Tong et al., 2021), *Ochotona youngi* (Tong et al., 2021), *Nyctereutes* sp., *Canis chihliensis* (Tong et al., 2012, 2021), *Homotherium* sp., *Acinonyx* sp., *Lynx* sp., *Panthera* sp., *Pachycrocuta licenti*, *Mammuthus trogontherii* (Tong, 2012; Tong and Chen, 2016; Chen and Tong, 2017; Tong et al., 2021), *Hipparion* sp., *Equus sanmeniensis*, *Coelodonta nihowanensis* (Tong and Wang, 2014), *Elasmotherium peii* (Tong et al., 2014, 2018), *Sus lydekkeri*, *Paracamelus gigas* (Tong et al., 2021), *Nipponicervus elegans* (Tong et al., 2021), *Eucladoceros boulei* (Tong and Zhang, 2019), *Elaphurus bifurcatus* (Tong et al., 2021), *Spirocerus wongi*, *Gazella sinensis*, *Ovis shantungensis*, *Megalovis piveteaui*, *Bison palaeosinensis* (Tong et al., 2017). Among the 25 taxa mentioned above, 23 of which once appeared in the classical Nihewan fauna (=Xiashagou fauna), which account for 92% of the SSMZ fauna.

In the SSMZ fauna, the dominant species include *Canis chihliensis*, *Mammuthus trogontherii*, *Equus sanmeniensis*, *Coelodonta nihowanensis*, *Sus lydekkeri*, *Eucladoceros boulei*, *Spirocerus wongi*, *Gazella sinensis* and *Bison palaeosinensis*, most of which have gotten published; the present paper is going to focus on the study of the small and medium-sized bovids, all of which are regarded as having the same geologic horizon.

The SSMZ site lies at the neighboring hill of Xiaochangliang, a well-known Paleolithic Site in Nihewan Basin. Based on the stratigraphic correlation in the field, the fossil-bearing sand-silt bed at SSMZ site is a little higher than the cultural layer at XCL site (Tong et al., 2011; Liu et al., 2012), whose paleomagnetic age is about 1.36 Ma BP (Zhu et al., 2001). On the other hand, the SSMZ fauna is very similar with the classical Nihewan fauna in faunal composition, which means the SSMZ fauna should have an approximate age as the latter based on faunal correlation (Tong et al., 2021), whose recent dating result is 2.2–1.7 Ma (Liu et al., 2012).

2 New fossil materials and the extant specimens compared

The information of all of the studied specimens from SSMZ is listed in Table 1. All of the fossils are reposited in IVPP.

The compared local extant antilopines include the following species as defined by Jiang (2004): *Gazella subgutturosa*, *Procapra picticaudata*, *P. gutturosa*, *P. przewalskii*, *Pantholops hodgsonii* and *Saiga tatarica*. The compared extant specimens are from the following collections: Institute of Vertebrate Paleontology and Paleoanthropology, CAS; Institute of Zoology, CAS; Northwest Institute of Plateau Biology, CAS.

Table 1 Studied fossil specimens of small to medium-sized bovids newly unearthed from SSMZ

Materials	Field No.	Catalog No. (IVPP)	Context information
Spirocerus wongi			
Partial skull with horn-cores	N-07-122	V 28650	E4-8
Juvenile maxilla with DP2–M1	N-06-135	V 28651	E13-5
Left mandible with dp2–m1	N-06-167	V 28652.1	E14-4
Partial right mandible with dp2–m1	N-06-178	V 28652.2	E14-4
Partial right mandible with p4–m3	N-16-046	V 28653	I20-12
Left Mc III+IV	N-11-209	V 28655	H20-9
Right naviculo-cuboid	N-11-042-2	V 28656.1	G21-7
The fused 2nd+3rd tarsals	N-11-042-3	V 28656.2	H20-9
The 1st tarsal	N-11-042-4	V 28656.3	G21-7
Right Mt III+IV	N-11-042-1	V 28656.4	G21-7
Gazella sinensis			
Partial skull with horn-cores	N-11-273	V 28657	H22-9
Partial skull with horn-cores	N-06-128	V 28658	E14-2
Partial skull with left horn-core	N-06-237A	V 28659.1	D10-6
Right horn-core	N-06-237B	V 28659.2	D10-6
Partial skull with right horn-core	N-06-166	V 28660	E14-4
Partial skull with right horn-core	N-08-04 (02)	V 28661	H15-2?
Partial skull with left horn-core	N-08-037	V 28662	H16-3
Partial skull with left horn-core	N-08-078	V 28663	G15-6
Partial skull with left horn-core	N-16-029	V 28664	I20-10
Partial skull with right horn-core	N-17-050	V 28665	J15-13
Partial skull with right horn-core	N-17-052	V 28666	J16-13
Partial skull with left horn-core	N-17-064	V 28667	I16-13
Left horn-core	N-07-60	V 28668	E16-11
Left horn-core	N-17-067	V 28669	J16-14
Partial skull with left horn-core	N-18-75	V 28670	I11-13
Partial skull with right horn-core	N-18-85	V 28671	I12-13
Partial skull with left horn-core	N-18-168	V 28672	K13-17
Partial maxilla with P3–M1	2007.9.1	V 28673	F19-1
Partial maxilla with M1–3	N-17-176	V 28674	K16-17
Partial right mandible with p2–m3	N-06-220	V 28675	E12-5
Partial left mandible with p2–p3, m1–3	N-06-222	V 28676	D12-5
Partial right mandible with p4–m3	N-08-048	V 28677	H15-4
Partial left mandible with p4–m3	N-08-068	V 28678	H16-4
Partial right mandible with p3–m3	N-08-067	V 28679	H16-4
Partial left mandible with p2–m3	N-08-069	V 28680	H15-5
Partial right mandible with p2, p4–m3	N-11-250-1	V 28681.1	F20-9
Partial left mandible with p2–m3	N-11-250-2	V 28681.2	F20-9
Left mandible with p3–m3	N-16-086	V 28682	K23-13
Partial left mandible with p4–m3	N-17-081	V 28683	I16-14
Partial right mandible with p4–m3	N-17-162	V 28684	K16-17
Left mandible with dp2–4, m1–2	N-17-164-g	V 28685.1	K16-17
Right mandible with dp2–4, m1–2	N-17-164-d	V 28685.2	K16-17
Partial mandible with p4–m3	N-17-177	V 28686	K16-17
Left humerus (distal)	N-11-174	V 28687	F20-9
Left Mc III+IV	N-15-050	V 28688	H30-3
3rd phalanx	N-15-028	V 28689	G29-4
Left naviculo-cuboid	N-15-125	V 28690	H30-6
Distal part of left tibia	N-15-246	V 28691	F30-3
Left astragalus	N-15-244	V 28692	G29-3

Continued

Materials	Field No.	Catalog No. (IVPP)	Context information
Ovis shantungensis			
Partial maxilla with left DP4–M1, right DP2–M1	N-07-069-A+B	V 28693	F17-1
Nearly complete left Mc III+IV	N-11-179	V 28694	H23-9
Megalovis piveteaui			
Left radius	N-16-051	V 28654	I20-12
Right Mc III+IV	N-17-017	V 28695	I17-10

3 Methods, terminology and abbreviations

The suprageneric classification of Bovidae is after Pilgrim (1939), Sokolov (1953), Gentry (1992, 2010), McKenna and Bell (1997), Vrba and Schaller (2000), Grubb (2001), Matthee and Davis (2001), Kuznetsova and Kholodova (2003), Hassanin et al. (2012); the taxonomy at generic level is after Groves (2014) and Castelló (2016); the classification of the local Antilopinae and Caprinae is after Jiang (2004).

The osteological terms are after Reshetov and Sukhanov (1979), Gee (1993), Brown and Gustafson (1979). The terms of tooth nomenclature are after Janis and Lister (1985), Gentry (1992, 2010), Bärmann and Rössner (2011). Upper case letters are used for upper, and lower case letters for lower teeth respectively.

The specimens were measured according to the methods used by von den Driesch (1976). The measurement of horn-core is after Young (1932) and Ratajczak et al. (2016). The measurements were taken with sliding calipers in millimeters. The internal structures of the horn-cores were examined by using the CT scan machine (450ICT) at IVPP.

The biochronological framework follows Tong et al. (1995) and Qiu (2006).

Institutional and locality abbreviations CAS, Chinese Academy of Sciences; GWL, Gongwangling; HPICR, Hebei Province Institute of Cultural Relics; IOZ, Institute of Zoology, CAS; IVPP, Institute of Vertebrate Paleontology and Paleoanthropology, CAS; MNHN, Muséum National d'Histoire Naturelle; NM, Nihewan Museum; NNNRM, Nihewan National Nature Reserve Management; NWIPB, Northwest Institute of Plateau Biology, CAS; OV, Prefix to the catalog numbers of extant specimens in IVPP; SIZ, Shaanxi Institute of Zoology; SSMZ, Shanshenmiaozui; TNHM, Tianjin Natural History Museum; V, Prefix in the catalog numbers for vertebrate fossils in IVPP; XCL, Xiaochangliang; XSG, Xiashagou; YS, Yushe.

Morphological abbreviations APD, anteroposterior diameter; TD, transverse diameter; Mc, metacarpal; Mt, metatarsal.

4 Systematic paleontology

4.1 Spiral-horned antelope

Class Mammalia Linnaeus, 1758

Order Artiodactyla Owen, 1848

Suborder Ruminantia Scopoli, 1777

Infraorder Pecora Linnaeus, 1758

Family Bovidae Gray, 1821

Subfamily Antilopinae Baird, 1857 (=Gazellinae Coues, 1889)

Tribe Antilopini Gray, 1821

Genus *Spirocerus* Boule & Teilhard de Chardin, 1928

***Spirocerus wongi* Teilhard de Chardin & Piveteau, 1930**

Materials See Table 1.

Skull bones: One partial adult skull (Fig. 2A) and one partial juvenile skull (Fig. 2B1–3) can be referred to the the species *S. wongi*. The adult one has very limited frontal bone, but with almost complete horn-cores of both sides. In front view, the frontal bone shows two moderately developed supraorbital pits which accommodate the two prominent supraorbital foramina which are connecting directly to the anterosuperior corner of the orbit and each has a very large internal opening, even larger than in an ox. The eye socket is very large and deep,

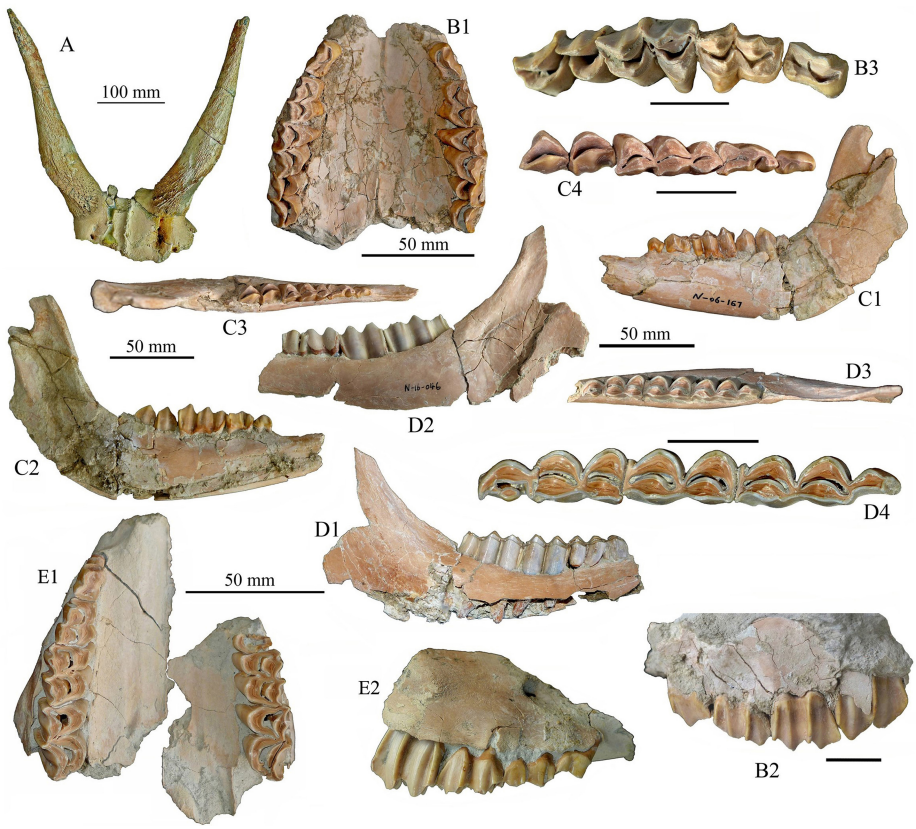

Fig. 2 Partial skulls, jaw bones and teeth of *Spirocerus wongi* (A–D) and *Ovis shantungensis* (E) from SSMZ A–D. *Spirocerus wongi*: A. partial skull with horn-cores (IVPP V 28650), B1–B3. juvenile maxilla with DP2–M1 (V 28651), C1–C4. left mandible with dp2–m1 (V 28652.1), D1–D4. partial right mandible with p4–m3 (V 28653); E1–E2. *Ovis shantungensis*, maxilla with left DP4–M1 and right DP2–4 and M1 (V 28693) A. anterior view; B1, E1. palatal views; B2, C1, D1, E2. buccal views; C2, D2. lingual views; B3, C3–4, D3–4. occlusal views. The unmarked scale bars equal 20 mm

and has a trench-like roof with flat superior wall rather than domed as in other taxa. The horn is very close to the orbit, which is only 30 mm apart; the postorbital constriction is also obvious. The cranial width at the horn bases is 149.0 mm, and the two horn-cores are 65.6 mm apart at the base. The frontal sinus (pneumatization) is also quite developed, but the diverticulum doesn't extend to the cornual process (Fig. 3A2).

Horn-core: The horn-core is a typical form of *Spirocerus wongi*, with rugose surface and only one spiral carena (or carène or keel) (Fig. 3B1–4), rather than two as in *S. peii* and *S. kiakhtensis*. The carena derives from the basal anterior part and heteronymously spirals upwardly (the left horn spirals anticlockwise but the right one spirals clockwise) and ends near the tip after finishing one complete revolution. The pedicle is quite short. The interior of the horn-core is nearly solid but with a complicated minor canal system (Fig. 3A1–2, C1–5), which resembles those of the true gazelles. The cross-section of the horn-core is elliptical (Fig. 3C1–5). Around the basal part of the horn-core, there are many nutrient foramina, among which the ones above the orbit are the largest (Fig. 3B2). The dimensions of the horn-cores are shown in Table 2.

Table 2 Measurements of the horn-cores of *Spirocerus wongi*, compared with related species (mm)

Dimensions	*S. wongi*	*S. wongi*	*S. wongi*	*S. peii*	*S. kiakhtensis*
	This paper	Teilhard and Piveteau (1930)	Bai et al. (2019)	Young (1932)	Dong et al. (2009)
Total length	283	290	264.3–353.8 (288.8)[&]	270	151–160. 9[#]
Diameter of horn-core base (APD)	64.0–64.2	57–60	51.6–80.2	55	35.9[#]
Latero-medial diameter of horn-core base (TD)	49.3–51.4		43.5–54.5		
Angle of divergence of horn-cores	50°	57°*	about 70°		50°[#]
Cranial width at the horn bases	149.0	144*	134.1		
Minimum distance between inner margins of horn processes	65.6	100*	51.7		64.2[#]
Distance between the supraorbital foramina (upper margin)	86.7	68.5*	63.2		

* Measured by the present authors from the figures of Teilhard de Chardin and Piveteau (1930); [&] calculated by the present authors; [#] juvenile individual.

Maxilla: One juvenile maxilla with DP2–4 and unfully erupted M1 on both sides (Fig. 2B1). Except the trench-like anterior part, the palatal surface is quite flat; the palatal widths between DP2, DP3, DP4 and M1 are 37.0, 47.1, 49.0 and 58.9 mm respectively.

Mandible: One partial adult mandible with p4–m3 (Fig. 2D1–4) and two juvenile partial mandibles (Fig. 2C1–4) are referred to the species *S. wongi*. The two juvenile mandibles (IVPP V 28652.1 and V 28652.2) should belong to the same individual because of their exactly similar dental features. One of the juvenile mandible (V 28652.1) retains most of the mandibular body and the ramus, but lacks the angular process and the tip of the coronoid process. The adult partial mandible has the mandibular condyle completely preserved. All the mandibular specimens have no speciality except the moderately pachyostosed mandibular body (Fig. 2C3, D3), which is similar with those of the extant sumatran serows (*Capricornis sumatraensis*).

Deciduous upper teeth (Fig. 2B3; Table 3): All of the deciduous upper cheek teeth are completely molarized except DP2. DP2 is elongated, but the posterior lobe is relatively reduced and the posterior fossette (or infundibulum) is shallow. The DP3 has much more wider but shorter posterior lobe relative to the anterior one, and the two fossettes are V-shaped in occlusal view; the mesostyle rib is quite pronounced, the lingual wall of the first lobe is roundish. The DP4 has a much more wider anterior lobe relative to the posterior one; the mesostyle rib is also quite pronounced; the lingual wall of the posterior lobe is more roundish relative to the anterior one. The metacone rib is less developed in all three kinds of tooth. The dimensions of the deciduous teeth are shown in Table 3.

Deciduous lower teeth (Fig. 2C1–4): The dp2 is less complicated; the crown has a rectangle outline but the front portion becomes slightly narrower; the paraconid is crest like; there is no parastylid; the protoconid is robust; the metaconid and hypoconid are equally developed; the entoconid is not developed. Between the protoconid and the metaconid, there exists a shallow valley. The dp3 is much more complicatedly constructed, and larger than dp2 (Fig. 2C4); the outline is in narrow trapezoid, with the lingual side concave and the narrow portion toward anterior; in front of the paraconid there is a parastylid; the metaconid is very elongated and extended backwards; the valley between parastylid and paraconid is closed, but the valley between the paraconid and metaconid is open; the buccal wall is flat but slightly convex, and the hypoflexid is quite shallow. The dp4 is the most complicated and longest tooth which has three lobes, each lobe has a separate infundibulum, namely anterior, posterior and third fossettid respectively, and the three lobes are nearly equally developed but the second one

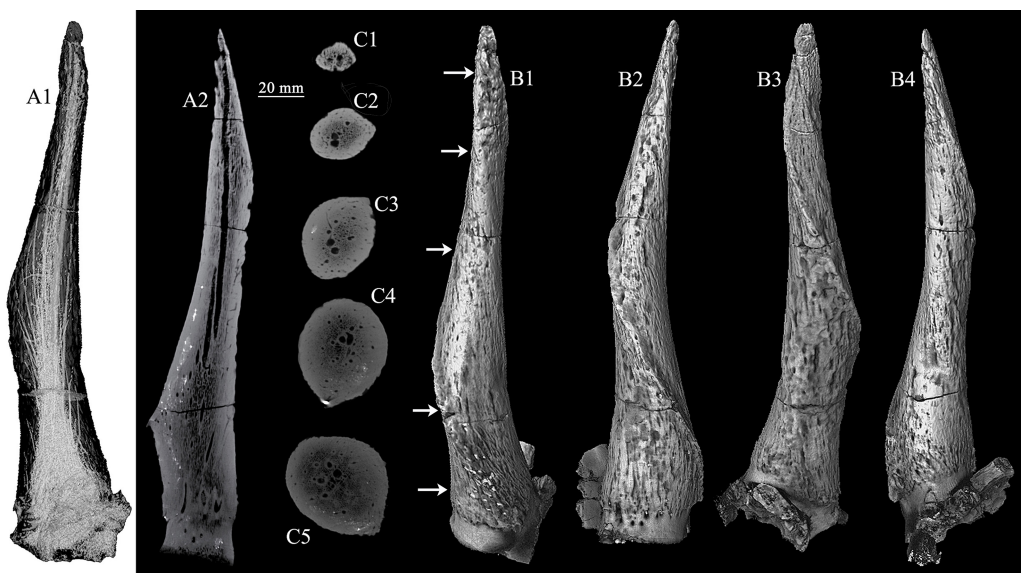

Fig. 3 CT scan images and 3-D reconstructions of the horn-core of *Spirocerus wongi* from SSMZ (IVPP V 28650)
A1–A2. CT scan images showing the general canal system (A1) and a longitudinal slice (A2);
C1–C5. CT scan slices showing the changes of cross sections and the canal system at different levels;
B1–B4. CT image reconstruction of the right horn-core
in anterior (B1), lateral (B2), posterior (B3) and medial (B4) views

is slightly more expanded; according to the nomenclature by Bärmann and Rössner (2011), the anterior lobe consists of anterobuccal conid and anterolingual conid, the middle lobe consists of protoconid and metaconid, and the posterior lobe is composed of hypoconid and entoconid respectively; on the buccal side, there is no basal pillars. The lingual cuspids, the parastylid, mesostylid and metastylid are well developed.

Permanent lower teeth (Fig. 2D1–4; Table 3): Only one partial mandible preserves p4 to m3. The p4 is very advanced in well developed protoconid and metaconid, but other cuspids are extremely reduced; metaconid is column-like but connects with paraconid mesially by a narrow bridge, it doesn't contact protoconid; there is a narrow and deep groove between metaconid and entoconid. The m1 and m2 are very similar in morphology, except the latter is longer and has more developed goat fold; the infundibulums are very narrow; the lingual cuspids are compressed linguobuccally and the lingual wall is quite flat. The m3 has three lobes, the front two of which are very similar to m2 in shape and size; the third lobe has no infundibulums and is linguobuccally compressed. From the lingual aspect, prominent parastylid and entostylid ribs on m2 and m3 can be seen, and even a rib at the linguo-distal corner of hypoconulid lobe can also be observed, but the mesostylid rib is only slightly developed at the top part of the crown. From the buccal view, no basal pillars can be observed.

Postcranial bones: See Table 1.

Table 3 Measurements of the teeth of *Spirocerus wongi*, compared with related species (mm)

Species		*S. wongi*	*S. wongi*	*S. wongi*	*S. peii*	*S. kiakhtensis*	*S. kiakhtensis*	*Ovis shantungensis*
Sources		This paper	Teilhard & Piveteau (1930)	Bai et al. (2019)	Young (1932)	Boule et al. (1928)	Dong et al. (2009)	This paper
DP2	L	14.2–14.5	13				10.5	9.5
	W	10–10.2	8				7.7	7.4
DP3	L	19.9–20.3	19–23				12.5	14.8
	W	13.6–14.2	10–12				11.1	12.8
DP4	L	23.5–23.7	22–24				16.5	18.0–18.5
	W	16.8–18.1	12				13.6	15.1–15.5
DP2–4	L	56.2–57.4	52				39.4	41.9
M1	L	26.6–26.7	19?				19.5–24.9	24.0–24.3
	W	15.3	15?				18.2–23.9?	15.7–15.8
dp2	L	10.5–10.8						
	W	6.6–6.7						
dp3	L	16.4–16.6						
	W	9.2						
dp4	L	28.2–28.5						
	W	11.3–11.6						
p4	L	13.6	13–15	17.1	12	15		
	W	8.4	9	8.3	9	9		
m1	L	17.9	13–20	17.2	15	25?		
	W	12.3	11–14	10.7	11	11		
m2	L	23.2	21–26	21.6	21	26		
	W	12.6	12–13	10.7	11.5	13		
m3	L	32.2	32	30.2	32			
	W	11.7	11–13	10.1	12			

Mc III+IV: The Mc III+IV (Fig. 4A1–3) is a kind of short but robust one, with the distal end expanded. The cranial aspect is more rounded on the shaft while the caudal surface is more flat. At both the proximal and distal ends the medial side or Mc III looks prominently thicker than the lateral side. In proximal view, there are two large articular facets, the larger facet or magnum trapezoid facet is relatively wide and has a curved edge, which is articulated with the fused 2nd and 3rd carpals; the smaller facet or unciform facet is triangular and articulates with the 4th carpal; between the two facets there exists a groove or depression. The posterior medial tubercle is not developed. In anterior view, the vascular groove (or metacarpal gully) is nearly unobservable and the nutrient foramen is tiny. In posterior view, the shaft has a quite flat surface, except near the proximal end, there is a depression; a small nutrient foramen exists near the distal articular surface. The dimensions are shown in Table 4.

Naviculo-cuboid (IVPP V 28656.1): Except the astragalus and calcaneum, a complete set of right tarsal bone was preserved, which still articulates with the metatarsal bones (V 28656.4) in situ. In proximal view, the articular surface consists of a large trochlear facet with a pair of depressions and a distinct posterior beak-like projection (or internal process) at the medioposterior corner, but the internal process is not developed; a narrow sloped belt-like facet occupies the lateroposterior part, which articulates with the calcaneum; there is a tiny foramen at the bottom of the lateral depression which corresponds with the lateral condyle of the distal trochlea of the astragalus. In distal view, the general outline of the distal surface is that of a rounded quadrilateral with two large anterior articular facets and two small posterior facets; the anteromedial facet is articulated with the fused 2nd and 3rd tarsals; the smallest facet articulates with the 1st tarsal; the other two lateral facets articulated with the Mt III+IV directly. In anterior view, the facet articulated with fused 2nd and 3rd tarsals is higher in position than other distal facets; the calcaneal facet is sloping upward anteroposteriorly. In posterior view, there is a large projection at the posteromedial corner; the posterior surface is not flat and with some small nutrient foramina; there exists a notch between the medial and the calcaneal facets, and the latter extends downward along the back wall (Fig. 4B4). The TD is 43.4 mm, and the APD is 43.8 mm.

The fused 2nd+3rd tarsals (IVPP V 28656.2) (Fig. 4B2–3): Its anatomical position is under the anteromedial portion of the naviculo-cuboid. The proximal articular facet is concave, but the distal facet is convex. Its form is anteroposterior elongated, and its greatest dimension is 29.5 mm.

The 1st tarsal (or medial cuneiform): Short and pillar-like, with facets at both ends; the navicular facet is larger but depressed, and the Mt III facet is smaller but flat. Its anatomical position should be under the beak-like projection of naviculo-cuboid (Fig. 4B2–3).

Mt III+IV (Fig. 4C1–3): In general view, the Mt III+IV has the very proximate length as the Mc III+IV, which is quite different from the common ungulates whose metatarsals are prominently longer than metacarpals belonging to the same individual; furthermore, the distal end expands more sharply relative to the shaft. In proximal view, the proximal surface

Table 4 Measurements of metacarpals of bovids from Nihewan Basin, compared with related taxa (mm)

Taxa	Sources	Length	Proximal width	Proximal APD	Distal width	Distal APD	Midshaft width	Midshaft APD	Index of stoutness (Distal width/total length) (%)
		Mc III+IV							
Bison palaeosinensis	Teilhard and Piveteau (1930)	231–248	72–74		65				28–29
	Tong et al. (2018)	226–233	60–67.8	35–38.6	59–63.5	34.2–34.7	36–39.5	26–27.6	26–28
Megalovis latifrons	Viret (1954)	200	56.5		60				30
Megalovis latifrons	Radulesco and Samson (1962)	192	56		64		35.7		33.3
Megalovis piveteaui	This paper	212	59	37	59	32	34	25	27.8
	Teilhard and Piveteau (1930); Schaub (1937); Radulesco and Samson (1962)	192–204	51–57		54–61				28–30#
Megalovis wimani	Schaub (1937)	185	52		57				30.8#
Ovis shantungensis	This paper	221	41	29	42	27	26	20	19
	Teilhard and Piveteau (1930)	231–233	42–44		42–44.5				18–19
Ovis ammon	Fedosenko and Blank (2005)	218							
Ovis shangi	Teilhard and Young (1936)	150	26		28		17		18.7
Spirocerus wongi	This paper	175	47	32	56	29	31	19	32
Spirocerus kiakhtensis	Sokolov (1959)	170			60.9#		35.0#	22.0#	35.8
Gazella cf. *G. lydekkeri*	Zhang and Yang (2016)	141							
Gazella sinensis	This paper	180	22	17	23	16	12.5	11.3	12.8
Gazella subgutturosa	Demircioglu and Ince (2020)	146.0(F)	18.4(F)		18.0(F)		10.5(F)	9.7(F)	
		150.7(M)	19.6(M)		18.9(M)		11.4(M)	9.9(M)	
Procapra przewalskii	Boule et al. (1928)	142			18–21				12.7–14.8
Procapra gutturosa	Boule et al. (1928)	180			23				12.8
Procapra gutturosa	This paper (OV 1124)	146	15.5	8.0	16.7	12.1	8.7	7.0	11.4
Saiga tatarica	Prat (1966b)	153	25	18.5	25.5		13.5		17.7
Capra ibex	Prat (1966a)	126–155	28.5–38.5	20.5–27	31.5–43	19–24	20–27.5		
		(139.2)	(33)	(23.8)	(36.7)	(21.3)	(23.8)		
Praeovibos priscus	Kahlke (1964)	193.7#							
Ovibos moschatus sussenbornensis	Kahlke (1961)	189.9#	62.8#	36.5#	69.1#		44#		36.4
		Mt III+IV							
Spirocerus wongi	This paper	173.0	36.9	34.0	45.3	26.1	22.0	21.5	26.2

Calculated by the first author of this paper; mean values in parentheses.

has a polygon outline, and consists of four articular facets; the two anterior facets are large and kidney-shaped, but the two posterior facets are small and elongated. The mediolateral dimension of the proximal end is slightly larger than the anteroposterior dimension. The two large articular facets meet at the front middle part but diverge posteriorly; both of them have longer anteroposterior dimensions. The anteromedial facet articulates with the fused 2nd and 3rd tarsals; the anterolateral facet articulates with naviculo-cuboid. There are two smaller facets located near the posterior margin. The posterolateral facet has larger mediolateral dimension and articulates with naviculo-cuboid. The small roundish facet articulates with the 1st tarsal. The dimensions are shown in Table 4.

Fig. 4 Postcranial bones of small and medium-sized bovids from SSMZ
A–C. *Spirocerus wongi*: A1–A3. left Mc III+IV (IVPP V 28655),
B1–B4. right naviculo-cuboid+lat-mid+medial cuneiforms (V 28656.2–3),
C1–C3. right Mt III+IV (V 28656.4); D–I. *Gazella sinensis*: D1–D3. partial left humerus (V 28687),
E1–E4. left Mc III+IV (V 28688), F. distal epiphysis of left tibia (V 28691),
G1–G2. left astragalus (V 28692), H1–H2. left naviculo-cuboid (V 28690), I1–I3. 3rd phalanx (V 28689);
J–K. *Megalovis piveteaui*: J1–J4. left radius (V 28654), K1–K4. right Mc III+IV (V 28695);
L1–L4. *Ovis shantungensis*: left Mc III+IV (V 28694). A1, C1, D1, E1, G1, J1, K1, L1. anterior views;
A2, B4, C2, D2, E2, G2, J2, K2, L2. posterior views; A3, B1, C3, E3, H1, J3, K3, L3. proximal views;
B2, D3, E4, F, H2, J4, K4, L4. distal views; B3. medial view; I1. lateral view; I2. interdigital view;
I3. volar view. The arrows indicate the lateral projection of the radius. The unmarked scale bars equal 20 mm

In posterior view, a very small nutrient foramen positioned slightly off-center some way under the posterior apophysis. Very shallow central trough only can be observed at the mid-shaft.

At the distal end, there are two distal condyles whose intercondylar margins are parallel. On the anterior surface, the vascular groove (or midline dorsal groove) is wide but shallow and opens to the intercondylar groove.

Comparison and discussion The degree and direction of horn-core torsion, the type of spiraling and the development and position of the keels are the crucial characters to classify the fossil spiral-horned antelopes (Kostopoulos, 2004). In the early publications, the torsion direction (clockwise or anticlockwise) always means for the right horn (Pilgrim, 1939). Moreover, the recent publications prefer to use “homonymous” and “heteronymous”, if the left horn twists clockwise, the horns are termed homonymous, or else it’s heteronymous.

Spirocerus was established by Boule and Teilhard de Chardin in 1928, and included the specimens from Sjara-osso-gol (=Salawusu) of Nei Mongol (Inner Mongolia) to it. Later on, the similar fossils from Nihewan (Teilhard de Chardin and Piveteau, 1930) and Yushe (Teilhard de Chardin and Trassaert, 1938) also were referred to this genus. *Spirocerus* was originally included into the subfamily Tragelaphinae by Teilhard de Chardin and Trassaert (1938), later on, it was referred to the subfamily Caprine (Sokolov, 1953); while currently it is usually placed in the subfamily Antilopinae (McKenna and Bell, 1997; http://taxonomicon.taxonomy.nl/TaxonTree.aspx?src=0&id=68446). More recent assignment is to Bovinae (Bai et al., 2019). Up to now, the classifications of *Spirocerus* at the species level are mainly based on horn-core characters, which caused quite a lot of confusions. Kahlke (1999) proposed that the most primitive *Spirocerus* with only anterior carena should be referred to *S. wongi*. Concerning the bicarinate forms with longer and slender horn-cores, the stratigraphically older ones can be referred to *S. kiakhtensis peii*, while the younger materials with correspondingly shorter and more massive horn-cores to *S. kiakhtensis kiakhtensis*. Moreover, all of the species of *Spirocerus* have heteronymous spiraled horns.

In China, three species were recognized, namely *S. wongi*, *S. peii* and *S. kiakhtensis*; the former one only has one spiral carena while the latter two have two spiral carenas on each horn-core (Teilhard de Chardin and Trassaert, 1938). This genus mainly limited to northern China, Trans-Baikal region and the central Asian countries. From *S. wongi* via *S. peii* to *S. kiakhtensis*, the size is getting smaller and the horn-cores are becoming straighter. Moreover, the current knowledge is mainly about the horn-cores, whereas the cranial features of the genus *Spirocerus* is still unknown; the dental and postcranial characters are still insufficiently studied yet, because no dentition was found attached to a skull with horn-cores in the fossil record. Relative to its cranial size, *Spirocerus* should have big postcranial bones, but the partial skeleton associated with skull materials of *S. kiakhtensis* discovered near Ulan-Ude of Russia showed that the limb bones of this kind of animals are quite short but robust; therefore, it was inferred that *Spirocerus* has big skull but short limbs and similar body-build as the extant muskox does (Sokolov, 1959).

It has to be indicated that the maxillary bone described by Teilhard de Chardin and Piveteau (1930:pl. XII, fig. 1) (current catalog No. NIH 136) should be rechecked, because it seems that the DP4 was mistaken as M1, which can be easily verified by a CT scanning. Furthermore, the Nihewan limb bones identified as *S. wongi* and Ovibovine gen indet. respectively by Teilhard de Chardin and Piveteau (1930) should be reconsidered; the metapodials referred to *S. wongi* (pl. XII: figs. 2 and 4) are too long, they should belong to *Ovis shantungensis*; the metapodials referred to Ovibovine gen indet. (pl. XIII: figs. 3 and 4) have the similar form and size as those of *M. piveteaui.* The metacarpal from SSMZ described in this paper has almost exactly the same form and same size as that of *S. kiakhtensis* from the Trans-Baikal region (Sokolov, 1959).

The lower teeth from SSMZ are different from those of Xiashagou in their slightly less developed goat folds and lack of the basal pillar in m1.

It's necessary to say that until now, none of the dental materials ever discovered for *S. wongi* was directly associated with the horns; that's to say all of the previous and current descriptions about the teeth of *S. wongi* can be open to questions. It's lucky enough that some cranial specimens of *S. kiakhtensis* have their horn-cores and teeth preserved jointly (Dong et al., 2009). These specimens are very crucial for the morphological studies of the extinct *Spirocerus*.

Spirocerus has developed frontal sinuses, but they do not extend to the horn-core at all (Fig. 3A2). According to Farke's paper of 2010, the frontal sinus doesn't always have phylogenetic significance. But the present authors think it's more important if the frontal sinus extends to the horn-core, i.e. if there is a cornual diverticulum of the frontal sinus or if the horn-core is hollowed.

Spirocerus is typical for its spiral and straight horn-cores, but sometimes it could be confused with *Antilospira zdanskyi*; some of the specimens (IVPP V 24483.4, V 25878.1–2) referred to *Spirocerus* (Bai et al., 2019) possibly belong to *Antilospira* or some other taxon because of their un-straight horn-cores and the different carena feature (with prominent groove alongside the spiral carena). Hermier et al. (2020) proposed that the horn-cores in *Antilospira* are variably inclined backwards and divergent but their surface usually shows much deeper longitudinal grooves. *Antilospira* is the most similar contemporaneous taxon with *Spirocerus*, and it was also uncovered in the Nihewan Basin, but it can be distinguished from the latter by the following characters: un-straight horn-cores, usually with two grooved and slowly twisting carenas (Teilhard de Chardin and Trassaert, 1938).

The comtemporaneous genus *Gazellospira* also has similar horn-cores, but it was only discovered in Europe and northern Asia not including China. Furthermore, *Gazellospira* has two spiraled keels of which the posterior one is the sharpest (Hermier et al., 2020), which are less straight as those of *Spirocerus*. On the other hand, the metapodials of *Gazellospira* are completely different from those of *Spirocerus*, the formers' are much longer and slender (Hermier et al., 2020; Vislobokova et al., 2020). Furthermore, the lower p4 of *Gazellospira* has

its lingual valleys open (Duvernois and Guérin, 1989), while the anterior valley is closed in *Spirocerus*. Although the intraspecific variations in cranial and postcranial features have been recognized between different sexes and different latitudes for *Gazellospira torticornis*, its horn-cores and metapodials as well as the lower p4 are distinctly different from those of *Spirocerus*.

The other comtemporaneous genus *Pontoceros* is typical for its homonymous torsion of horn-core, which is different from other Early Pleistocene spiral-horned antelopes, including *Tragelaphus*, *Gazellospira* and *Spirocerus* (Vislobokova and Titov, 2020).

Concerning the taxonomic position of the extinct *Spirocerus*, it's still controversial. Its large supraorbital foramina (generally sunken in large frontal depressions) and horn-core characters (straight, solid, moderately spaced, twisted clockwise and situated directly over the orbits) support an attribution to the subfamily Antilopinae, but its solid and quite divergent horn-core, lack of post-cornual fossa, short but stout metapodials and the limb proportions share more similarities with the ovibovines under the subfamily Caprinae. Sokolov (1959) postulated that the extinct *Spirocerus* should have a similar appearance as muskox (*Ovibos*). It's a pity that the fossil records for this animal are too few to reach a definite phylogenetic approach currently. Although some recent publication attributed *Spirocerus* to the subfamily Bovinae Gill, 1872 (Bai et al., 2019), it seems that few morphological characters can support this proposal.

4.2 Chinese gazelle

Genus *Gazella* Blainville, 1816

***Gazella sinensis* Teilhard de Chardin & Piveteau, 1930**

Materials See Table 1.

Skull bones: One partial adult skull (Fig. 5B1–3) and one partial juvenile skull (Fig. 5A) can be identified as *Gazella sinensis*. The adult specimen has partial frontal bone preserved, but with almost complete horn-cores of both sides. In front view, the frontal bone has two large supraorbital foramina which are situated in triangular-shaped depressions of the frontals (supraorbital pits) near the base of the horn pedicels and closely above the orbit, they connect directly to the eye socket and have big roundish internal openings. At the lateroposterior aspect of the basal part of the pedicle, there exists a post-cornual fossa (Fig. 5D2, 6A1). The wall of the cranial bone is very thin (Fig. 5B3). The dimensions are shown in Table 5.

Horn-core: The general characters of the horn-cores are short but with moderately long pedicle, without torsion of their axes, and the surface is decorated with longitudinal grooves or striate. In anterior view the two horns are straight and are nearly sub-parallel, i.e. the divergence angle is small (16º–22º) (Fig. 5A, B1, B3); in lateral view they have a gentle backward curvature (Fig. 5D2, E). The horn-cores are solid interiorly but with many longitudinal canals, most of which open upwardly (Fig. 6A1'–A4', B1'–B3'); at the basal part adjacent to the pedicle, there are a few large foramina and the one just above the post-cornual fossa is the largest (Fig. 6A4', B3'). The horn-core has a sub-circular cross section with slight transverse compression (Fig. 6A1'–A4'). The horn-cores vary in size (Fig. 5; Table 5) and the

development of longitudinal grooves, which may be subject to gender and age difference. The dimensions of the horn-cores are shown in Table 5.

Mandibles: There is no peculiarity in the mandibles. They have short symphyseal length but long diastema between lower canine and p2. The mental foramen is large and lies at the midway of the diastema at the buccal aspect, but sometimes an extraordinary mental foramen will occur below p3. The mandibular depth is shallow under the premolars but becomes deep rapidly as it passes back from beneath the premolars to the molars. The angular process is moderately developed. The coronoid process is long and recurved backward distally. The mandibular condyle is highly superior to dentition. Mandibular foramen is small and the maximum height of opening is at the same horizontal level as the alveolar margin (Fig. 7C3).

Upper teeth: Only two specimens with upper teeth (IVPP V 28673 and V 28674) can be assigned to the species *G. sinensis*. All of the upper cheek teeth are less hypsodont. The P3 is very special in its tendency of molarization by the appearing posterior infundibulum and has greater length than width (Fig. 7A; Table 6). The P4 has only one lobe but without any peculiarity except its developed styles. Each molar consists of two lobes constructed by paracone and protocone, metacone and metaconule respectively; in M1 and M2, the anterior lobe usually has larger width (buccolingual dimension), but in M3 the anterior lobe is narrower than the posterior one. The infundibulum has simple structure and the fold can be seen only in M3. No basal pillar can be observed (Fig. 7A–B).

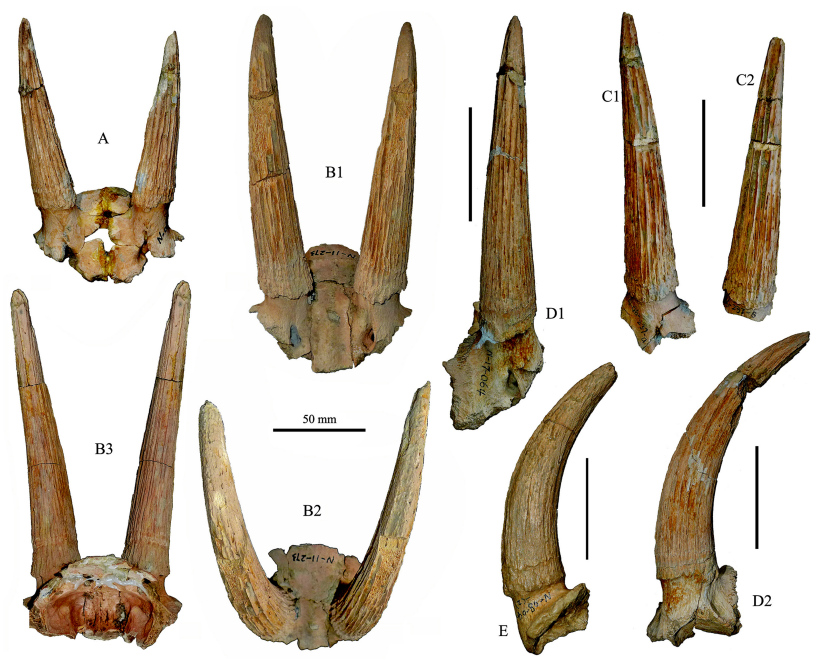

Fig. 5 Incomplete skulls and horn-cores of *Gazella sinensis* from SSMZ

A. partial skull of a juvenile with horn-cores (IVPP V 28658); B1–B3. partial skull with horn-cores (V 28657); C1–C2. left and right horn-cores (V 28659.1, V 28659.2); D1–D2. partial skull with left horn-core (V 28667); E. partial skull with right horn-core (V 28661). A, B1, C1–2, D1. anterior views; B3. posterior view; B2. dorsal view; E. medial view; D2. lateral view. The unmarked scale bars equal 50 mm

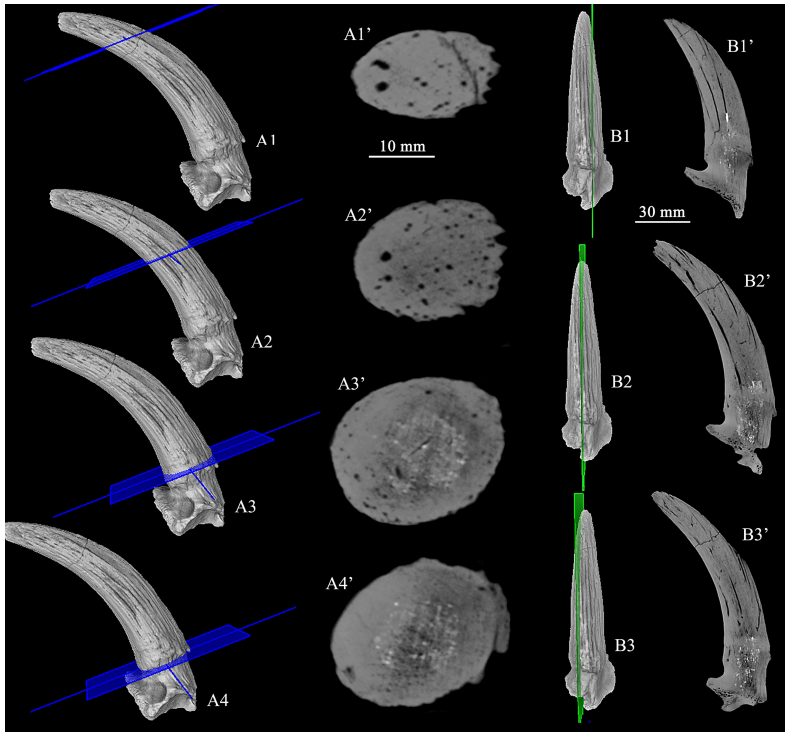

Fig. 6 CT scan images of the the horn-core of *Gazella sinensis* (IVPP V 28661) from SSMZ
A1–A4. CT image reconstruction showing postions of the cross CT scan slices (A1'–A4');
B1–B3. CT image reconstruction showing postions of the longitudinal CT scan slices (B1'–B3')

Lower teeth: The lower premolars are less hypsodont than those of the caprinines, but complicatedly constructed, except p2 which is simply constructed and prominently smaller than the other two (Table 6). Lower p3 and p4 has the similar structure, both of them are elongated but p3 has the lingual wall open both mesially and distally (Fig. 7C4, D1, G–H), sometimes with the anterior valley partially closed (Fig. 7D1; 8A); on the other hand, the p4 only has the posterior valley open, like a narrow groove (Fig. 7C4, D3, F–J; 8A) and coincides with the type 5 of p4 patterns proposed by Janis and Lister (1985). Each premolar has two roots. Lower molars are elongate and with developed goat folds, but lack basal pillars; m1 and m2 are very similar in size and shape; m3 has three lobes, but the third lobe has very shallow infundibulum. Molars are quite hypsodont. The m1 and m2 with two roots, but m3 has three roots.

Lower deciduous teeth: The deciduous teeth are brachyodont (Fig. 7E2). The dp2 resembles p2 in shape; dp3 is similar with p3; while dp4 is similar with m3 in having three lobes but is different in having a larger third lobe and with a basal pillar at the buccal groove between the second and the third lobe (Fig. 7E3).

Postcranials: A humerus with partial shaft and complete distal end preserved, the length of the remained part is 73.9 mm (IVPP V 28687) (Fig. 4D1–3). In anterior view, the indentation (radial or coronoid fossa) above the articular surface is shallow; the medial edge of the trochlea is curved and with the upper portion inclined laterally; at the lateral two-fifths

Table 5 Measurements of partial cranial bones and horn-cores of *Gazella sinensis* (mm)

	IVPP V 28657	V 28658	V 28659.1	V 28659.2	V 28660	V 28661	V 28662	V 28665	V 28667	V 28670	V 28671	V 28672
Greatest breadth across orbits: ectorbitale-ectorbitale	>81.8	>80.9										
Width between supraorbital foramina	30.9	35.0										
Frontal angle	34°											
Angle of divergence of horn-cores	16°	22°										
Width between horns	65.8	66.6										
Minimum distance between inner margins of horn processes	23.2	29.0										
Diameter of horn-core base (APD)	28.4	24.9	26.3	26.6	27.2	27.0	27.7	25.3	28.2	25.9	27.6	24.7
Latero-medial diameter of horn-core base (TD)	21.3	19.5	21.3	21.4	21.3	20.8	20.4	19.6	21.7	19.8	21.4	17.5
Full curved length of horn-core	170	118	146	135	130	132	135	>101	152	131		
Straight length of horn-core	160	110	132	123	120	117	120	>95	140	116		

part of the trochlear surface, there exists a sagittal ridge whose lower part is nearly vertical but with the upper part slightly inclined laterally; the lowest part of the distal articular surface occurs at the lateral side; there is a longitudinal trench at the middle part of the articular surface; below the articular surface at the medial side, the medial epicondyle can be observed. In posterior view, the shaft has a very straight medial margin and a nutrient foramen at the lateral aspect can be seen; the olecranon fossa at the distal end is very deep; the medial epicondyle extends much more downward than the lateral one. The distal APD is 27.3 mm; the distal TD is 29.7 mm.

Mc III+IV: A complete left Mc III+IV (IVPP V 28688) (Fig. 4E1–4). In general, the bone is very slender; the cranial aspect is more rounded on the shaft and the caudal aspect is much flatter and slightly concave at the upper part; the distal epiphysis is not fused yet. In proximal view, there are two articular facets, the larger one or magnum trapezoid facet is prominently wider and deeper, which articulates with the fused 2nd and 3rd carpals; the smaller one or unciform facet is oval-like and is the articular surface for 4th carpal; between the two facets there exists a narrow ridge; no nutrient foramen can be observed at the proximal end (Fig. 4E3). In anterior view, a prominent tubercle (extensor carpi radialis insertion: Gentry, 1966: fig. 12) occurs at the cranial aspect of the proximal end; no vascular groove (or metacarpal gully) can be observed, while the nutrient foramen is clear but small and located near the epiphyseal suture; the widest portion lies at the epiphyseal suture rather than at the trochlea (Fig. 4E1). In posterior view, no prominent groove can be observed except the upper part; the articular facet for the vestigial 5th metacarpal is absent. A prominent nutrient foramen exists near the epiphyseal suture and a tiny nutrient foramen occurs at the mid-shaft (Fig. 4E2). The dimensions are shown in Table 4.

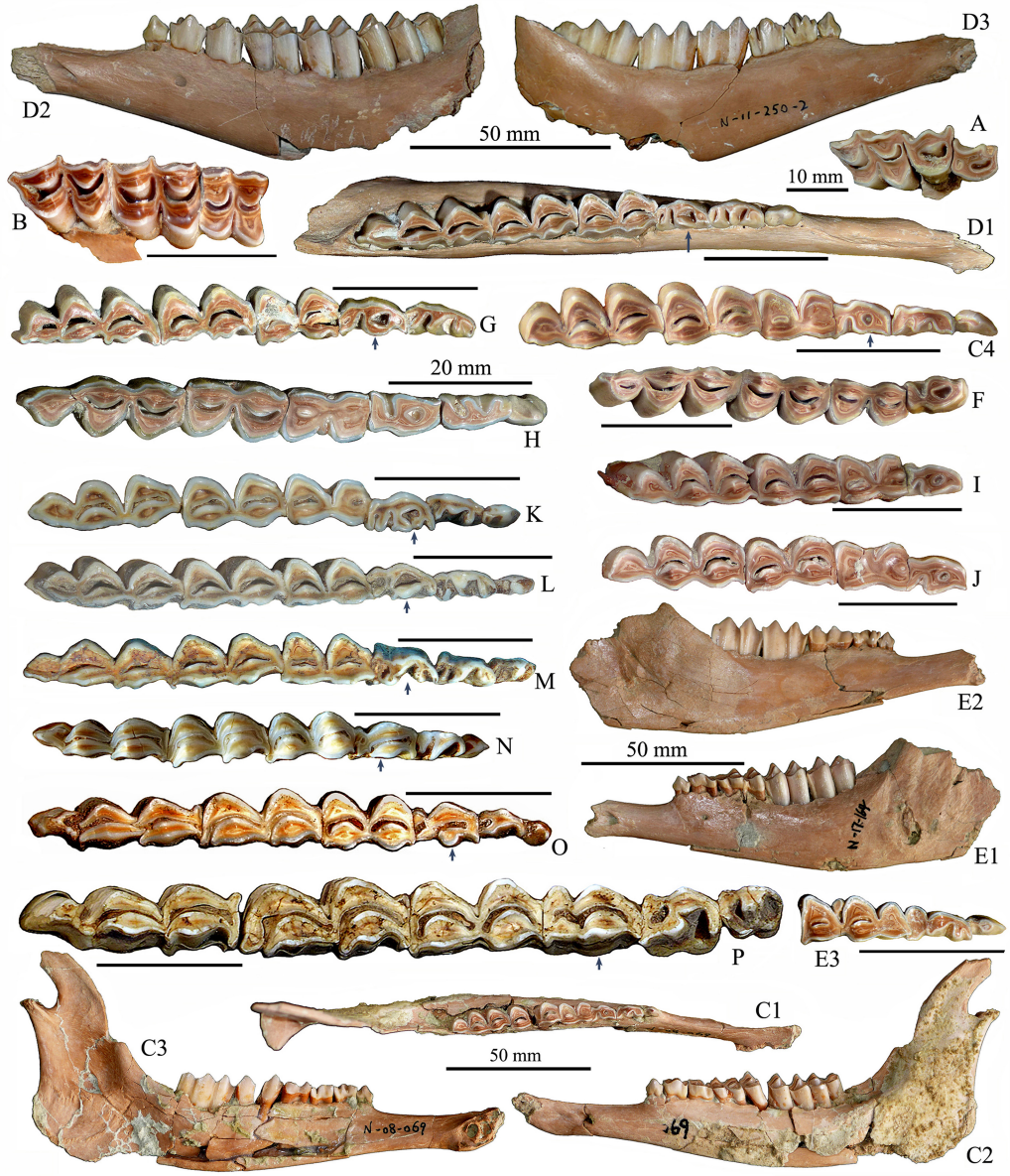

Fig. 7 Jaw bones and teeth of *Gazella sinensis* from SSMZ (A–J), compared with related taxa (K–P)
A. maxilla with P3–M1 (IVPP V 28673); B. maxilla with M1–3 (V 28674);
C1–C4. left mandible with p2–m3 (V 28680); D1–D3. left mandible with p2–m3 (V 28681.2);
E1–E2. left mandible with dp2–4 and m1–2 (V 28685.1), E3. detail of dp2–4; F. right p4–m3 (V 28677);
G. left p3–m3 (V 28682); H. right p2–m3 (V 28675); I. left p4–m3 (V 28686); J. left p4–m3 (V 28678);
K. *Procapra przewalskii*, right p2–m3 (horizontally flipped) (NWIPB-0001172♀);
L. *Procapra gutturosa*, left p2–m3 (NWIPB 620032); M. *Gazella subgutturosa*, left p2–m3 (NWIPB 609001);
N. *Pseudois nahaur*, left p2–m3 (NWIPB-KX1); O. *Capra ibex*, left p2–m3 (IOZ-2);
P. *Ovis ammon*, left p2–m3 (OV 1346-2). A, B, C1, C4, D1, E3, F–P. occlusal views;
C2, D2, E1. buccal views; C3, D3, E2. lingual views. The arrows indicate the variations of p4
The unmarked scale bars equal 20 mm

Table 6 Measurements of teeth of *Gazella sinensis* from SSMZ, compared with those from Xiashagou (mm)

IVPP V		28675	28676	28673	28674	28677	28678	28679	28680	28681.1 (r)	28681.2 (l)	V 28682	28683	28684	28685.1 (l)	28685.2 (r)	28686	Teilhard & Piveteau (1930)
P3	L			6.9														
	W			6.4														
P4	L			8.3														
	W			7.8														
M1	L			11.0	9.8													
	W			10.9	12.7													
M2	L				13.4													
	W				12.9													
M3	L				15.1													
	W				10.3													
M1–M3	L																	38–45
dp2	L														5.2	4.9		
	W														2.5	2.5		
dp3	L														8.5	7.5		
	W														4.3	3.5		
dp4	L														12.9	13.8		
	W														5.4	5.3		
dp2–dp4	L														26.4	27.1		
p2	L	5.3	5.6						6.0	6.4	5.8							
	W	3.0	3.7						3.1	3.2	3.1							
p3	L	8.2	8.4					9.1	8.4		8.3	9.6						
	W	3.9	4.2					3.8	4.4		4.2	4.5						
p4	L	8.6				8.7	8.5	7.9	8.1	8.9	8.7	9.7		7.8			7.9	
	W	4.5				5.1	5.1	4.5	4.3	4.7	4.7	5.0		4.6			5.0	
p2–p4	L	22.2					22.3	20.8	21.5	22.5	22.4							22–28
m1	L	10.1	10			11.5	10.2	10.6	10.0	11.3	12.9	11.5	9.4	10.3	13.4	13.7	10.1	
	W	5.9	6.5			7.2	6.8		6.6	6.6	6.7	7.8	5.2	7.1	6.8	6.8	7.1	
m2	L	12.1	12.0			14.2	12.5	11.9		13.6	13.8	13.4	11.8	13.0	14.9	15.4	12.6	
	W	7.2	7.0			7.7	7.5	7.8	7.2	7.1	7.1	8.0	7.7	7.7	6.9	6.9	7.8	
m3	L	19.4	19.1			21.9	19.0	19.2	18.6	20.3	20.2	19.4	19.4	19.2			20.1	
	W	7.3	7.5			7.2	7.5	7.6	7.5	7.3	7.1	7.7	7.2	7.9			7.6	
m1–m3	L	41.8	42.5			46.1	43.1	41.7		46.4	45.7	44.9	39.5	41.9			41.2	43–50
p2–m3	L	64.1	64.0			64.2	66.8	67.0	<67.8	69.1	69.4							65–78

Distal epiphysis of tibia: On the distal end (IVPP V 28691) (Fig. 4F), the articular grooves are nearly parallel to the sagittal plane of the shaft, the medial groove is narrow but longer, the lateral groove is wide but shorter; between the two grooves, there exists a sagittal ridge, and the anterior end of the ridge is beak-like and distally projected; at the anteromedial corner, there is a long projection. There are two small articular surfaces on the lateral edge for the attachment of the lateral malleolus (or distal fibula). The APD is 18.5 mm, the TD is 21.3 mm.

Astragalus: A complete astragalus (IVPP V 28692) is preserved (Fig. 4G1–2). In anterior view, there are two proximal trochlear ridges (or condyles), which are parallel to each other and to the sagittal plane, the lateral ridge is prominently higher and wider. Between the two proximal trochlear ridges, there exists a deep trench-like median groove. The lateral border of the trochlear condyles is straight. The distal trochlea also consists of two parts, between them is a shallow saddle-like groove. In posterior view, the posterior articular surface for calcaneum is flat to slightly convex, but with a shallow longitudinal medial groove; the lateral edge is nearly straight; the medial bottom extends further downward and becomes confluent with the distal trochlear surface. The lateral face is trench-like and with anterior and posterior rims; the anterior rim extends upward and beak-like; at the bottom, the facet for calcaneum is oval-shaped. On the medial aspect, there is no articular facet. The length is 29.2 mm, the width is 17.2 mm.

Naviculo-cuboid: A complete naviculo-cuboid bone (IVPP V 28690) is preserved (Fig. 4H1–2). In proximal view, two articular surfaces can be observed, one for astragalus, the other for calcaneum; the former consists of a pair of depressions and a distinct posterior beak-like projection (or internal process) at the medioposterior corner; the latter is a narrowly sloped belt-like facet occupies the lateroposterior part; there is a tiny foramen at the bottom of the lateral depression. In distal view, the general outline is that of a rounded quadrilateral with two larger anterior articular facets and two smaller posterior facets. The anteromedial facet is articulated with the fused 2nd and 3rd tarsals; the smallest facet articulates with the 1st tarsal; the other two lateral facets articulated with the Mt III+IV. In anterior view, there is a large projection at the posteromedial corner, which is separated from other part by a deep notch; the facet articulated with the fused 2nd and 3rd tarsals is higher in position than other distal facets; the posterior surface is not flat. The APD is 21.6 mm, and the TD is 22.3 mm.

The 3rd phalanx: One complete distal (or 3rd or ungula) phalanx (IVPP V 28689) (Fig. 4I1–3) was unearthed, whose general look is quite narrow. In lateral view, both the dorsal and plantar margins are nearly straight except a slight concave at the middle part of the plantar margin. In proximal view, the dorso-posterior corner is projected; the articular surface can be divided into two facets, which articulate with distal end of 2nd phalanx. In distal view, the plantar surface is nearly flat and triangular and with the acute angle toward the anterior.

Comparisons and discussions Premolars are crucial for taxonomic identification for the gazelles, especially the tooth structures of the lower p4 which is usually regarded as the

most practical tooth in taxonomic distinctions (Boule et al., 1928; Teilhard de Chardin and Piveteau, 1930; Gentry, 1966; Janis and Lister, 1985; Chen, 1997). Among all the *Gazella* species, including both extant and fossil forms, the lower p4 usually has open lingual valleys (Teilhard de Chardin and Piveteau, 1930; Teilhard de Chardin and Trassaert, 1938; Zhang and Yang, 2016; Li et al., 2018) (Fig. 7M, 8E), except *G. sinensis* (Fig. 7C4, D3, F–J; 8A) and *G. yushensis* Chen, 1997; whereas the *Capra* species usually has the anterior valley closed in p4, i.e. paraconid and metaconid joined to form a continuous anterolingual wall (Fig. 7O), and the posterior valley sometimes is also closed. Among all the *Gazella* species, *G. sinensis* has the most complicated lower p3, some of which have the anterior valleys partially closed lower in crown, and all the cuspids and stylids are well developed, especially the parastylid is very robust, and the metaconid is the most developed relative to other compared Asian gazelles' (Fig. 8A); but most p3s have their lingual valleys open. Because of the preorbital fossa, the fossils represented by *G. sinensis* were included into the genus *Gazella*; on the other hand, its lower p4 has closed anterior valley, which is a crucial character of *Procapra*; therefore, the species *G. sinensis* was considered as the direct ancestor of *Procapra* (Sokolov and Lushchekina, 1997).

In addition to lower p4, there exist other crucial premolar characters to distinguish the gazelle taxa in China, e.g. *Saiga tatarica* usually lacks and *Pantholops hodgsonii* exclusively lacks p2 in their dentitions (Fig. 8F–G).

The toothrow length is rather stable than their cranial sizes among the extant gazelles in China (Fig. 9: raw data from Jiang, 2004); although the Mongolian gazelle (*Procapra gutturosa*) is remarkably larger in body size and cranial length than others, its toothrow length has no prominent difference. Therefore, it seems impossible to distinguish the small gazelles only based on their toothrow lengths (Fig. 9); in addition, the blue sheep also has similar tooth-row length with the gazelles; while the wild goat has slightly larger tooth-row length and the sheep has obviously larger tooth-row length than others (Fig. 7P).

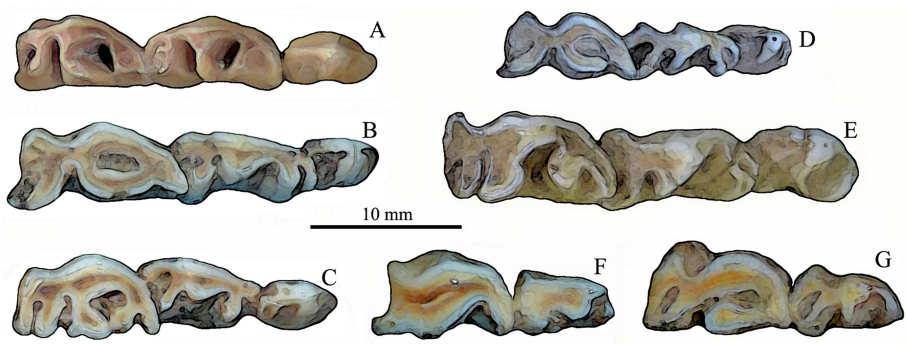

Fig. 8 Comparison of premolar series among some Quaternary gazelle species of China
A. *Gazella sinensis*, left p2–4, IVPP V 28681.2, SSMZ; B. *Procapra gutturosa*, left p2–4, NWIPB 0006065, extant; C. *P. przewalskii*, right p2–4 (horizontally flipped), NWIPB 0001172, extant; D. *P. picticaudata*, left p2–4, NWIPB 0001179, extant; E. *Gazella subgutturosa*, left p2–4, IVPP-c-05, extant; F. *Saiga tatarica*, right p3–4 (horizontally flipped), NWIPB S-80503, extant; G. *Pantholops hodgsonii*, left p3–4, NWIPB 77001, extant. All are in occlusal views

Furthermore, the horn-cores are highly uniform among the gazelle species, neither the size (Boule et al., 1928: table 13) nor the form can be used independently for specific distinctions. Although the post-cornual fossa of the frontal bone is also a common character among the gazelle species under the genera *Gazella* and *Procapra* in China, both fossil and extant, while it's absent in the species of *Saiga* and *Pantholops*, that's to say post-cornual fossa can be used for taxa distinction only to some extent. *Pantholops* is also different from other gazelles by its obviously smaller supraorbital foramen. Up to now, no fossil records of *Saiga* and *Pantholops* have ever been reported in China.

It's worth mentioning that the upper P3 has some kind of peculiarity in its tendency of molarization, which is a general phenomenon only occurs in some kinds of gazelle taxa, such as *G. subgutturosa* and the species of *Procapra* as well as the fossil forms of *Gazella*. In p4 morphology, *G. sinensis* is closer to *P. przewalskii.*

Concerning the horn-cores of gazelles, they are fairly uniform, not only in size, but also in form and interior structures, and usually have grooved surfaces and are nearly completely interiorly solid, i.e. without cornual diverticulums; therefore, it's almost impossible to distinguish the gazelle taxa only by horn-cores. On the contrary, the horn-cores of caprines are exclusively hollowed and diversified in shape.

The recent study in frontal sinuses and cranial pneumaticity of the bovid species shows a strong phylogenetic correlation with sinus morphology, except few exceptions (Farke, 2010). The extant species of *Procapra* has no frontal sinus, which is distinctly different from the *Gazella* species.

The metacarpal bone is prominently larger than such allied taxa, as *Gazella subgutturosa* and *Procapra przewalskii*, but with the same size as that of *P. gutturosa* (Table 4); in morphology, it has no peculiarity. The metapodial bone does have distinctive characters relative to those of the caprines in their extremely slenderness. Meanwhile, the BT (maximum breadth of trochlea) of the metacarpal of SSMZ specimen is 20.9 mm, which stands between those of the *Gazella* (15.1–20.1) and *Procapra* (21.5–21.6) (Wang et al., 2020).

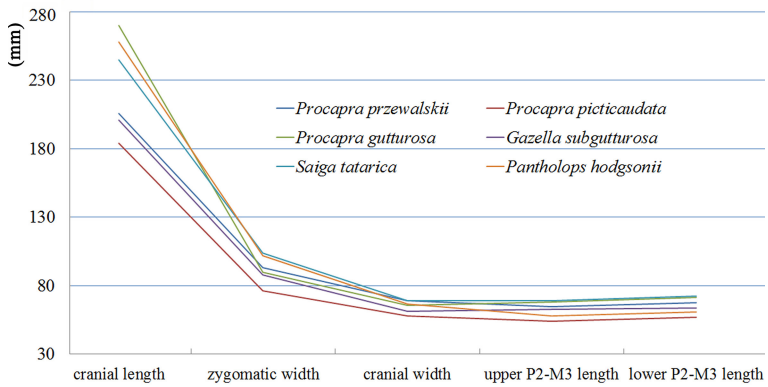

Fig. 9 Toothrow length and cranial size of extant gazelles in China
Raw data was employed from Jiang, 2004

Gazelles are adapted to open and arid environment, therefore, their range, both fossil and extant, only limited to the northern part in China, and the southernmost occurrences are Xuchang Man site at Lingjing in Henan Province (Dong and Li, 2008) and the Tuozi Cave in Jiangsu Province (Dong et al., 2007) (Fig. 1). As to the "*Gazella kaihuaensis*" from Zhejiang Province (Jin et al., 1994), it's an incorrect identification because of the following evidences: larger size, lack of a pedicle, horn far away from orbit, horn-cores with smooth surface rather than with longitudinal grooves, supraorbital foramen too small, small angle between horn-core and cranial roof, none of which coincides with the characters of a *Gazella*. The partial skull bone described by Jin et al. (1994) should belong to a serow (*Capricornis*).

4.3 Shandong sheep

Subfamily Caprinae Gill, 1872

Tribe Caprini Gray, 1821

Genus *Ovis* Linnaeus, 1758

***Ovis shantungensis* Matsumoto, 1926**

1930 *Spirocerus wongi*, Teilhard de Chardin and Piveteau, p. 71, Pl. XII, figs. 2 and 4

Maxilla: One maxilla with left DP4–M1 and right DP2–M1 (IVPP V 28693) (Fig. 2E1–2) can be referred to *Ovis shantungensis*. The DP2 is deeply worn and the infundibulum has disappeared. The DP3 is moderately worn, with robust paracone and metacone as well as metaconule, the protocone is less developed, with robust parastyle, the posterior lobe is wider than the anterior one. The DP4 has equally developed main cusps, and the styles are also equally developed; the paracone rib is very robust, the anterior lobe is wider than the posterior one. In form, the M1 is very similar with DP4, but much bigger and more hypsodont. The dimensions of the teeth are shown in Table 3.

Metacarpal: One almost complete Mc III+IV is available (IVPP V 28694) (Fig. 4L1–4). The peculiarity is its slendness, which is really unuasal for a caprine taxon. In morphology, size and proportions, it's very similar with the metacarpal of a medium-sized deer, except its less developed vascular groove and less concave midshaft posterior surface. The two large proximal articular facets form an asymmetric semicircular, between them there is a groove which opens postwardly, but the nutrient foramen in the groove is tiny. The metacarpal gully is weak; the situation of the lower nutrient foramen is unclear because of the breakage; the cranial side is more rounded. In posterior view, the shaft has a shallow but broad longitudinal depression at the upper three-fifths of the bone, and the surrounding area is quite rugose, the lower part has quite flat posterior surface; a small nutrient foramen occurs near the distal trochlea. The greatest length is 221 mm, which is very close to that of *O. ammon* (218 mm) (Fedosenko and Blank, 2005); the BT (maximum breadth of trochlea) of the metacarpal of SSMZ is 39.3 mm, which falls within the range of *O. ammon* (30.1–41.9 mm) (Wang et al., 2020).

Comparisons and discussions The DP2 and DP3 have the similar form and size as the

counterparts of *O. shantungensis* from XSG (Teilhard de Chardin and Piveteau, 1930:text-fig. 26-B), but the M1 is prominently larger than the type specimen (Matsumoto, 1926). Compared with the deciduous teeth of *S. wongi*, Teilhard de Chardin and Piveteau (1930:text-fig. 26) had indicated their differences: *S. wongi* has much bigger and more elongated teeth, especially the DP3 and DP4; furthermore, it's also different from *O. shantungensis* in its faint cingulum-like structure at the antero-lingual part of DP3, the buccal wall is broad and flat, the lingual wall of DP2 is concave at the posterior lobe.

According to the data of metapodials of various *Ovis* species, both fossil and extant, it seems wrong assignments of the metatarsal bones from Yushe Basin to *Ovis* cf. *shantungensis* (Teilhard de Chardin and Trassaert 1938:83), and from Zhoukoudian Loc.1 to *Ovis* sp. (Young, 1932:76), because their total lengths are only 135 and 144 mm respectively, which are too short for an *Ovis* species.

4.4 Piveteau's giant sheep

Tribe Ovibovini Gray, 1872

Genus *Megalovis* Schaub, 1923

***Megalovis piveteaui* Schaub, 1937**

1930 Ovibovine gen. indet., Teilhard de Chardin and Piveteau, p. 76–79, Pl. XIII, fig. 2, 2a, 3–4

1942 ?*Budorcus* sp., Teilhard de Chardin and Leroy, p.82

Radius: A nearly complete left radius (IVPP V 28654) is preserved (Fig. 4J1–4). The radius is quite massive, the body is anteroposteriorly compressed, and with the middle portion curved anteriorly. The most peculiarities lie at the two ends: the proximal end consists of three glenoid sub-fossae, which are increasing in size from lateral to medial; the proximal articular surface of the glenoid fossa has an expanded and rounded medial outline; a deep V-shaped notch occurs at the middle fossa, which articulates with the ulna. The distal end is expanded, but the articular facet is moderate in size; a pronouced and rugose ulna facet lies at the posterolateral corner, which has a sharp projection toward the lateral side (indicated by an arrow in Fig. 4J4), which is a peculiarity of *Ovibos* (Gromova, 1960); the distal ulna is not fused to the radius. The total length is 271 mm, the proximal width is 64.5 mm, the proximal depth is 35.0 mm, the distal width is 61.0 mm, the distal depth is 42.2 mm.

Metacarpal: A right anterior canon bone (Mc III+IV) (IVPP V 28695) (Fig. 4K1–4). In general, both the proximal and distal ends expand to some extent, and the metacarpal bone is moderately stout. At both proximal and anterior aspects, the medial side or Mc III looks noticeably thicker than the lateral side. The two proximal articular facets are quite flat, and a narrow groove occurs between the facets. In anterior view, the shaft is roundish, and the vascular groove (or metacarpal gully) is very narrow at the upper par but widened around the nutrient foramen. In posterior view, the proximal portion of the shaft has a medial longitudinal depression, but the lower part is flat; a prominent nutrient foramen exists near the articular surface. The dimensions are shown in Table 4.

Comparisons and discussions Based on the fossils identified as Ovibovine gen. indet. by Teilhard de Chardin and Piveteau (1930), the species *Megalovis piveteaui* was established by Schaub in 1937; both the maxillary and the metacarpal bones are very similar with the species *Megalovis wimani* Schaub, 1937, but slightly larger.

The genus *Megalovis* of the Villafranchian are thought by many to be similar to the ancestral form of *Ovibos*, if not directly ancestral (Crégut-Bonnoure, 1984). Actually, Teilhard de Chardin and Piveteau (1930) had indicated the close affinity of *Megalovis piveteaui* with *Ovibos* in the following aspects: cheek teeth without basal pillars, premolars quite hypsodont (Fig. 10A), upper molars with small enamel loops between the lobes at the lingual side (Fig. 10B). Furthermore, the present authors also think the upper molars are quite elongated in crown and the upper premolars with spurs (Fig. 10B). Although the cranial and cornual features are almost completely unknown, the close relationship between *Megalovis* and ovibovines is verified. On the other hand, the metapodials of *Megalovis* are also quite stout (Table 4), which resembles those of the recent *Ovibos*.

Because of the poor fossil records, the knowledge about the features of *Megalovis* in China is very fragmented. The species *Megalovis guangxiensis* Han, 1987 was established based on partial jaw bones and isolated teeth from the Liucheng *Gigantopithecus* Cave in Guangxi. The striking differences between the species and other *Megalovis* species from the Palearctic Region lie in its extremely larger size and developed basal pillars as well as the dental cementum; the m3 basal length of *M. guangxiensis* can be as large as 50 mm (Han, 1987), which almost represents the largest bovid tooth ever discovered in China. The present authors suggest that the fossils once attributed to the species *M. guangxiensis* should be reconsidered, not only because they are too different from the normal *Megalovis* species both in size and form, but also for the far distance between them.

The teeth of *Megalovis* can be easily distinguished from those of *Spirocerus* and *Ovis*

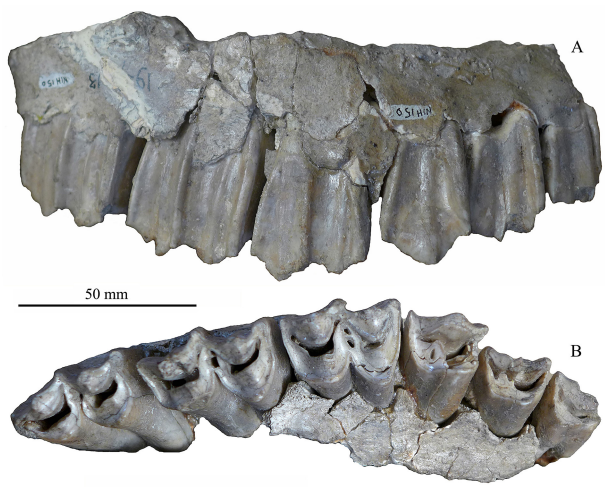

Fig. 10 Maxilla of *Megalovis piveteaui* (MNHN-NIH 150) from Xiashagou of Nihewan
A. buccal view; B. occlusal view

shantungensis in the same fauna by the characters as mentioned above; in size, they are prominently larger than those of the two latter taxa.

Concerning the other two contemporaneous local genera of Ovibovine, *Boopsis* and *Budorcas*, they are also poorly represented in the fossil record. It's difficult to go any further to make an intensive comparison among them.

Moreover, the SSMZ metacarpal bone has the most similar dimensions with those of *M. piveteaui* from XSG in Nihewan (Teilhard de Chardin and Piveteau, 1930) except its slightly larger size, but with almost the same stoutness index (Table 4).

5 Discussions

5.1 Distinctions of metapodial bones

The bovid metacarpal bones unearthed at SSMZ site are quite diversified, and most of them are easy to be identified according to their size and proportion, whereas some of them are very similar to each other both in size and stoutness. Therefore, an index should be employed, that's the robusticity index or stoutness index. Concerning the robusticity index, there exist two calculation methods: one is the relative dimensions of mediolateral diaphysis width and maximum length (SD/GL) ×100) (Maniakas and Kostopoulos, 2017), the other is the distal width/total length (Sher, 1997). Because it's easier and more practical to measure the distal width, this paper follows Sher's (1997) method to calculate the robusticity index, i.e. (distal width/greatest length) ×100. Based on the morphological observations and robusticity index calculations, the metacarpal bones of bovids from SSMZ site are quite clearly distinguished (Table 4; Fig. 11).

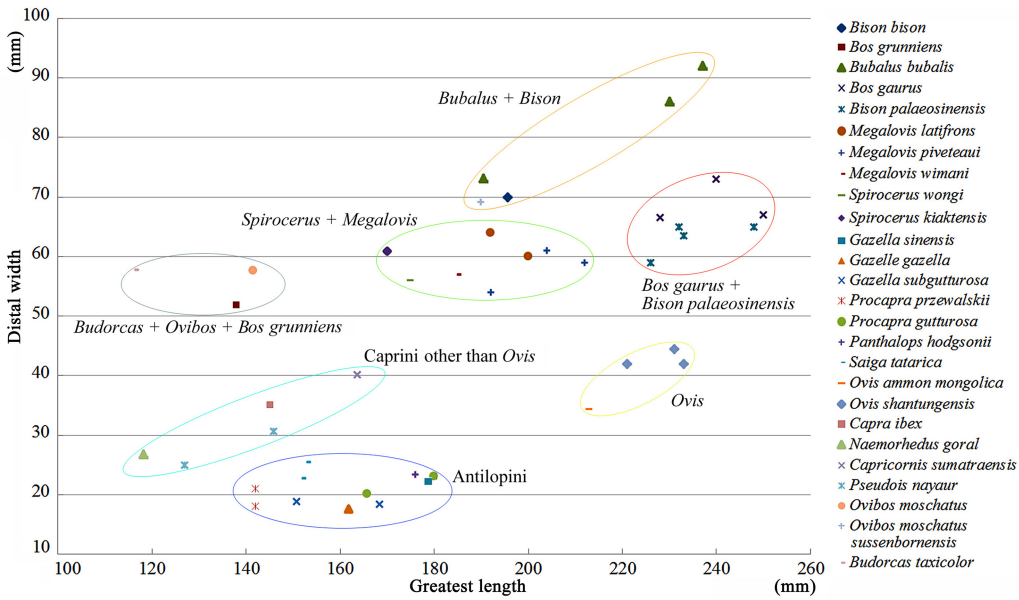

Fig. 11 Length VS distal width of metacarpal bones of diverse bovids
The data un-included in Table 4 are from Colbert and Hooijer, 1953; Scott, 1985

The metacarpal bone of *Spirocerus wongi* is the shortest and stoutest one, which is one of the crucial characters of the ovibovine taxa. In regard to the metapodial characters, it seems that *Spirocerus* has a closer affinity with the ovibovines rather than with the antilopines; Whereas almost all of the current publications place the genus *Spirocerus* within the subfamily Antilopinae or even within the tribe Antilopini together with *Gazella* and other gazelles.

The metacarpals of the allied taxa, *Gazellospira torticornis* and *Pontoceros ambiguous*, from Russia (Vislobokova et al., 2020) are much longer than those of the species of *Spirocerus*.

Megalovis piveteaui and *Bison palaeosinensis* have quite similar metacarpals both in size and proportion, the only difference is that the formers' is slightly smaller. Moreover, the Nihewan specimens of *M. piveteaui* share the similar size and form with *M. latifrons* of European (Viret, 1954; Radulesco and Samson, 1962) (see Table 4). *Megalovis* was referred to Ovibovini, maybe its metacarpal is the largest, but less stout, among the ovibovine taxa. *M. piveteaui* should be larger than *Spirocerus wongi* in body mass.

The metacarpal bone of *Gazella sinensis* is the most slender one among the bovid metacarpals in SSMZ fauna. The metacarpal specimens for the Pleistocene gazelle species are very rare in China, there is only one example up to date, i.e. the metacarpal of a Late Pleistocene *Procapra przewalskii* from Sjara-osso-gol, whose length is only 142 mm, but the counterpart of the extant *Procapra gutturosa* is 180 mm (Boule et al., 1928). Therefore, it can be estimated that the body mass of *G. sinensis* is similar with that of a *P. gutturosa*, and larger than *P. przewalskii* and the Late Miocene species *Gazella* cf. *G. lydekkeri* whose metacarpal's length is only 141 mm (Zhang and Yang, 2016).

The slenderness and total length of the metacarpal of *Ovis shantungensis* is very similar with that of a medium-sized deer, which is much longer and slender than those of the other Caprinae taxa, such as *Pseudois* and *Capricornis* as well as *Capra.*

For the extant ovibovines, the metapodials are exclusively short and robust, but for the extinct taxa, their metapodials are completely unknown except *Megalovis*, which is much longer than the counterparts of the living ovibovines. In quite a number of genetic studies, *Naemorhedus* and *Capricornis* were grouped with *Ovibos* (Hassanin et al., 2012), which makes the forms of the subtribe Ovibovina much diversified.

5.2 The bovid assemblage of the SSMZ fauna and its chronological significance

In China, Nihewan Basin and Yushe Basin are the most important fossiliferous spots for Late Cenozoic bovids, but the latter's bovid fauna is much more diversified (Teilhard de Chardin and Trassaert, 1938) than the former's. In Yushe Basin of Shanxi Province, the late Cenozoic deposits were subdivided into three biostratigraphical zones from bottom to top: Zone I, Zone II and Zone III (Licent and Trassaert, 1935; Teilhard de Chardin and Trassaert, 1938; Tedford et al., 1991); the Zone III shares almost all of its faunal members with the Nihewan fauna. In regard to the bovid taxa, only the advanced and relict ones of each group of Yushe Basin also appear in the Nihewan Basin; the relict elements include *Gazella*, *Antilospira*

and *Megalovis*; the newly appeared taxa include *Spirocerus*, *Ovis* and *Bison*. The recently discovered fauna in Jinyuan Cave in Dalian of Liaoning Province bears a very similar bovid assemblage (Jin et al., 2021) with the Nihewan fauna.

In the Nihewan Basin, except *Gazella* cf. *subgutturosa*, all the bovid taxa of the XSG fauna also occur in the SSMZ fauna. Furthermore, the mandible of Antilope gen. indet. of the XSG fauna (Teilhard de Chardin and Piveteau, 1930:68, fig. 25) was reidentified as *Hydropotes* by Tong et al. (2021).

In the SSMZ fauna, *Gazella sinensis* is the richest in fossil specimens, most of which are horn-cores and mandibles. *Spirocerus wongi* are better represented than the previous reports, especially its metapodials represent the first discovery. For *Megalovis piveteaui*, radius is the first time to be reported. Except a metacarpal bone, no other new anatomic elements were discovered for *Ovis shantungensis*.

Among the spiral horned antelopes, *Spirocerus wongi* shares the same chronology with *Antilospira* of the local area and *Gazellospira* species of central Asia and Europe, which is the Late Pliocene to the Early Pleistocene and no younger than 1.6 Ma (Hermier et al., 2020).

The *Ovis shantungensis* in Nihewan Basin used to be regarded as the earliest record of *Ovis* until the recent reports of the Early Pliocene *Ovis* sp. from Udunga in the Trans-Baikal region of Russian Siberia (Vislobokova et al., 1995; Vislobokova, 2008). The horn-cores of *O. shantungensis* are less stout than the later *O. ammon* (Bohlin, 1938), and it's almost certain that *O. shantungensis* indicates an Early Pleistocene age.

Moreover, the Nihewan fauna and other Early Pleistocene faunas in northern China correspond with a stage of decline of the spiral-horned antelopes and the rise of the hollowed-horn caprines (with developed horn-core sinuses or cornual diverticulum) and the appearing of large bovids (Bovini) and the ovibovines (Ovibovini).

Furthermore, the bovid assemblage of the Nihewan fauna indicates an open prairie or steppe dominated environment.

6 Conclusions

The small and medium-sized bovid fossils from Shanshenmiaozui site were identified as *Spirocerus wongi*, *Gazella sinensis*, *Ovis shantungensis* and *Megalovis piveteaui* respectively. The spiral-horned antelope was referred to *S. wongi* based on its twisted and with only one anterior keel of the horn-core; *S. wongi* has short but stout metapodials as does the species *S. kiakhtensis*; the cranial and horn-core characters of *Spirocerus* support a closer relationship with antilopines, while the metapodials share more similar traits with ovibovines. The species *G. sinensis* is typical for its lower p4 which is different from that of *G. subgutturosa* and earlier *Gazella* species in its exclusively closed anterior valley, and it is different from the *Procapra* species in its exclusively open posterior valley, no matter how narrow it is. Although *O. shantungensis* is poorly represented in the SSMZ fauna, the metacarpal bone is the first time

to be recognized. The present study shows that *O. shantungensis* has much longer metapodial bones than other caprine taxa do. *M. piveteaui* is also poorly represented in the fossil record, but it has very typical lower p4 and robust metacarpal bone; both characters support a closer affinity of *Megalovis* to ovibovines. Among the postcranial bones, the metapodials, especially the metacarpal bones are crucial not only for taxonomic identification, but also for phylogenetic and paleoecological reconstructions. The Shanshenmiaozui fauna shares 92% of its elements with that of the classical Nihewan fauna, which means they should have the similar geologic age, i.e. 2.2–1.7 Ma BP.

Acknowledgements The authors wish to express their thanks to the following people and organizations for their help: Wei Q, Han F, Sun B Y, Lü D, Sun J J, Xu Z J, Qiu Z W, Wang Q Y, Sun B H, Hu N, Liu X T and Yin C for participating the excavations; Xie F of HPICR, Li H Q of NNNRM and Hou W Y of NM for helps during excavations; Zheng M of TNHM, Argot C of MNHN, Li W J of NWIPB and Zhu X C of IOZ for providing access to collections; Qiu Z X, Zhou Z H, Vislobokova I A, van der Made J, Titov V, Salvagno L, Davis S J M, Jiang Z G, Zhang Z Q, Bai W P, Shi Q Q, Wang Y R and Wang J for sharing bibliographies and/or for fruitful discussions. Hou Y M for CT scanning. Thanks are also due to the two reviewers, Kostopoulos D S and Dong W, for their insightful questions and comments. The Editor-in-Chief and the editors contributed a lot to the improvement of the article. This work was supported by the following grants: the National Natural Science Foundation of China (Grant Nos. 42172021, 41572003), the Strategic Priority Research Program of Chinese Academy of Sciences (Grant No. XDB26000000) and the National Key R & D Program of China (Grant No. 2020YFC1521500).

泥河湾盆地山神庙咀遗址早更新世中–小型牛科动物化石新材料

同号文[1,2,3] 张 贝[4] 陈 曦[5] 王晓敏[6]

(1 中国科学院古脊椎动物与古人类研究所，中国科学院脊椎动物演化与人类起源重点实验室 北京 100044)

(2 中国科学院生物演化与环境卓越创新中心 北京 100044)

(3 中国科学院大学 北京 100049)

(4 北京自然博物馆 北京 100050)

(5 南京师范大学 南京 210023)

(6 中国社会科学院考古研究所 北京 100710)

摘要：山神庙咀是泥河湾盆地新发现的早更新世遗址，该遗址产出丰富多样的哺乳动物化石，其中包括如下属种的中–小型牛科动物：翁氏转角羚羊(*Spirocerus wongi*), 中国羚羊

(*Gazella sinensis*), 山东绵羊(*Ovis shantungensis*)和皮氏巨羊(*Megalovis piveteaui*); 中国羚羊是其中化石最丰富者。前两种化石主要以角心和头骨及下颌为主，此外，4个种都有掌骨和/或蹠骨发现。依据角心特征不难将有关类别鉴定到种一级，而对于牙齿及头后骨骼而言，要想确切鉴定是有一定困难的。在头后骨骼中，掌、蹠骨最值得关注，它不仅对属种鉴定有重要价值，而且对重建系统演化关系及解释古生态适应都是重要证据。修正了前人错误鉴定的泥河湾牛科动物的掌、蹠骨。山神庙咀动物群中的牛科动物以羚羊和野牛为主，表明泥河湾盆地在早更新世期间以草原环境为主导。

关键词：泥河湾山神庙咀，早更新世，中–小型牛科动物，新化石

References

Bai W P, Dong W, Zhang L M et al., 2019. New material of the Early Pleistocene spiral horned antelope *Spirocerus* (Artiodactyla, Mammalia) from North China and discussion on its evolution. Quat Int, 522: 94–102

Bärmann E V, Rössner G E, 2011. Dental nomenclature in Ruminantia: towards a standard terminological framework. Z Säugetierkd, 76(6): 762–768

Bohlin B, 1938. Einige Jungtertiäre und Pleistozäne Cavicornier aus Nord-China. Nova Acta Reg Soc Sci Upsala, Ser IV, 11(2): 1–54

Boule M, Breuil H, Licent E et al., 1928. Le Paléolithique de la Chine. Arch Inst Paléontol Hum, Mém, 4: 1–138

Brown C L, Gustafson C E, 1979. A key to postcranial skeletal remains of cattle/bison, elk, and horse. Rep Invest Wash State Univ, Lab Anthropol, 57: 1–199

Castelló J R, 2016. Bovids of the World: Antelopes, Gazelles, Cattle, Goats, Sheep, and Relatives. Princeton: Princeton University Press. 1–664

Chen G F, 1997. The genus *Gazella* Blainville, 1816 (Bovidae, Artiodactyla) from the Late Neogene of Yushe Basin, Shanxi Province, China. Vert PalAsiat, 35(4): 233–249

Chen X, Tong H W, 2017. On the hindfoot bones of *Mammuthus trogontherii* from Shanshenmiaozui in Nihewan Basin, China. Quat Int, 445: 50–59

Colbert E H, Hooijer D A, 1953. Pleistocene mammals from the limestone fissures of Szechuan, China. Bull Am Mus Nat Hist, 102(1): 1–134

Crégut-Bonnoure E, 1984. The Pleistocene Ovibovinae of western Europe: temporo-spatial expansion and paleoecological implications. Biol Pap Univ Alaska Spec Rep, 4: 136–144

Demircioglu I, Ince N G, 2020. Three-dimensional modelling of computed tomography images of limb bones in gazelles (*Gazella subgutturosa*). Anat Hist Embryol, 49: 695–707

Dong W, Li Z Y, 2008. Late Pleistocene Artiodactyla (Mammalia) from the Lingjing site, Xuchang, Henan Province (China). Vert PalAsiat, 46(1): 31–50

Dong W, Fang Y S, Zhang Z H, 2007. Artiodactyla Owen, 1848. In: Fang Y S, Dong W eds. The Early Pleistocene Mammalian Fauna at Tuozi Cave, Nanjing, China. Beijing: Science Press. 85–129

Dong W, Fu R Y, Feng X W et al., 2009. Late Pleistocene mammalian fauna from the Mashandong, Chaoyang, Liaoning Province. Acta Anthropol Sin, 28: 95–109

Driesch A von den, 1976. A guide to the measurement of animal bones from archaeological sites. Bull Peabody Mus, 1:

1–137

Duvernois M-P, Guérin C, 1989. Les Bovidae (Mammalia, Artiodactyla) du Villafranchien supérieur d'Europe occidentale. Geobios, 22: 339–379

Farke A A, 2010. Evolution and functional morphology of the frontal sinuses in Bovidae (Mammalia: Artiodactyla), and implications for the evolution of cranial pneumaticity. Zool J Linn Soc, 159: 988–1014

Fedosenko A K, Blank D A, 2005. *Ovis ammon.* Mamm Spec, 773: 1–15

Gee H, 1993. The distinction between postcranial bones of *Bos primigenius* Bojanus, 1827 and *Bison priscus* Bojanus, 1827 from the British Pleistocene and the taxonomic status of *Bos* and *Bison*. J Quat Sci, 8(1): 79–92

Gentry A W, 1966. Fossil Antilopini of East Africa. Bull Br Mus Nat Hist Geol, 12(2): 45–106

Gentry A W, 1992. The subfamilies and tribes of the family Bovidae. Mamm Rev, 22(1): 1–32

Gentry A W, 2010. Chapter 38: Bovidae. In: Werdelin L, Sanders W J eds. Cenozoic Mammals of Africa. Berkeley: University of California Press. 747–803

Gromova V, 1960. A Key to the Large Long Bones of Mammals. (Liu H Y trans). Beijing: Science Press. 1–162 (in Chinese; original work published in 1950 in Russian)

Groves C, 2014: Current taxonomy and diversity of crown ruminants above the species level. Zitteliana B, 32: 5–14

Grubb P, 2001. Review of family – group names of living bovids. J Mammal, 82(2): 374–388

Han D F, 1987. Artiodactyla fossils from Liucheng *Gigantopithecus* Cave in Guangxi. Mem Inst Vert Paleontol Paleoanthropol, Acad Sin, 18: 135–208

Hassanin A, Delsuc F, Ropiquet A et al., 2012. Pattern and timing of diversification of Cetartiodactyla (Mammalia, Laurasiatheria), as revealed by a comprehensive analysis of mitochondrial genomes. Compt Rend Biol, 335: 32–50

Hermier R, Merceron G, Kostopoulos D S, 2020. The emblematic Eurasian Villafranchian antelope *Gazellospira* (Mammalia: Bovidae): new insights from the Lower Pleistocene Dafnero fossil sites (northern Greece). Geobios, 61: 11–29

Janis C M, Lister A, 1985. The morphology of the lower fourth premolar as a taxonomic character in the Ruminantia (Mammalia; Artiodactyla), and the systematic position of *Triceromeryx*. J Paleontol, 59(2): 405–410

Jiang Z G, 2004. Przewalski's Gazelle. Beijing: China Forestry Publishing House. 1–251

Jin C Z, Wang Y, Liu J Y et al., 2021. Late Cenozoic mammalian faunal evolution at the Jinyuan Cave site of Luotuo Hill, Dalian, Northeast China. Quat Int, https://doi.org/10.1016/j.quaint.2021.01.011

Jin X S, Wu W T, Du T M, 1994. The discovery and study of Gazelle skull fossil in Zhejiang. Geol Zhejiang, 10(2): 1–4

Kahlke H D, 1961. Revision der Säugetierfaunen der klassischen deutschen Pleistozän-Fundestellen von Süßenborn, Mosbach und Taubach. Geologie, 10: 493–532

Kahlke H D, 1964. Early Middle Pleistocene (Mindel/Elster) *Praeovibos* and *Ovibos*. Comment Biol, 26(5): 1–17

Kahlke R D, 1999. The history of the origin, evolution and dispersal of the Late Pleistocene *Mammuthus-Coelodonta* faunal complex in Eurasia (large mammals). Rapid City: Fenske Companies. 1–219

Kostopoulos D S, 2004. Revision of some Late Miocene spiral horned antelopes (Bovidae, Mammalia). Neues Jahrb Geol Palaeont Abh, 231(2): 167–190

Kuznetsova M V, Kholodov M V, 2003. Revision of phylogenetic relationships in the Antilopinae Subfamily on the basis of the mitochondrial rRNA and β-Spectrin nuclear gene sequences. Dokl Biol Sci: Proc Acad Sci USSR, Biol Sci Sect, 391(1-6): 333–336

Li Y K, Shi Q Q, Chen S K et al., 2018. "*Gazella*" (Mammalia: Bovidae) from the Late Miocene Qingyang area, Gansu, China. Palaeont Electron, 21.2.24A: 1–27, https://doi.org/10.26879/838

Licent E, Trassaert M, 1935. The Pliocene lacustrine series in central Shansi. Bull Geol Soc China, 14: 211–220

Lister J A, 1985. The morphology of the lower fourth premolar as a taxonomic character in the Ruminantia (Mammalia; Artiodactyla), and the systematic position of *Triceromeryx*. J Paleontol, 59(2): 405–410

Liu P, Deng C, Li S et al., 2012. Magnetostratigraphic dating of the Xiashagou Fauna and implication for sequencing the mammalian faunas in the Nihewan Basin, North China. Palaeogeogr Palaeoclimatol Palaeoecol, 315: 75–85

Maniakas I, Kostopoulos D S, 2017. Morphometric-palaeoecological discrimination between *Bison* populations of the western Palaearctic. Geobios, 50: 155–171

Matsumoto H, 1926. On a new fossil race of bighorn sheep from Shantung, China. Sci Rep Tôhoku Imp Univ, Ser 2 (Geol), 10: 39–41

Matthee C A, Davis S K, 2001. Molecular insights into the evolution of the Family Bovidae: a nuclear DNA perspective. Mol Biol Evol, 18(7): 1220–1230

McKenna M C, Bell S K, 1997. Classification of Mammals Above the Species Level. New York: Columbia University Press. 1–631

Pilgrim G E, 1939. The fossil Bovidae of India. Palaeontol Ind New Ser, 26(1): 1–356

Prat F, 1966a. Les capridés. In: Lavocat R ed. Atlas de Préhistoire. Tome III. Faunes et flores préhistoriques de l'Europe occidentale. Paris: N. Boubée et cie (L'Homme et ses origines). 279–322

Prat F, 1966b. Les antilopes. In: Lavocat R ed. Atlas de Préhistoire. Tome III. Faunes et flores préhistoriques de l'Europe occidentale. Paris: N. Boubée et cie (L'Homme et ses origines). 323–336

Qiu Z X, 2006. Quaternary environmental changes and evolution of large mammals in North China. Vert PalAsiat, 44(2): 109–132

Radulesco C, Samson P, 1962. Sur la présence de *Megalovis latifrons* dans le Villafranchien d'Olténie (Roumanie). Vert PalAsiat, 6(3): 262–269

Ratajczak U, Shpansky A V, Malikov D G et al., 2016. Quaternary skulls of the saiga antelope from eastern Europe and Siberia: *Saiga borealis* versus *Saiga tatarica* – one species or two? Quat Int, 420: 329–347

Reshetov V, Sukhanov V B, 1979. Postcranial skeleton. In: Sokolov V E ed. European Bison—Morphology, Systematics, Evolution, Ecology. Moscow: Nauka Publishers.142–173

Schaub S, 1937. Ein neuer Cavicornier aus dem Oberpliocaen von Honan. Bull Geol Inst Univ Upps, 27: 25–31

Scott K M, 1985. Allometric trends and locomotor adaptations in the Bovidae. Bull Am Mus Nat Hist, 179: 197–288

Sher A V, 1997. An early Quaternary bison population from Untermassfeld: *Bison menneri* sp. nov. In: Kahlke R-D ed. Das Pleistozän von Untermassfeld bei Meiningen (Thüringen), Teil 1. Monogr Romisch-German Zentralmus Mainzer, 40(1): 101–180

Smith A T, Xie Y, 2008. A Guide to the Mammals of China. Princeton: Princeton University Press. 1–576

Sokolov I I, 1953. A primer of natural classification of Cavicorns (Bovidae). Proc Zool Inst Acad Sci USSR, 14: 1–295

Sokolov I I, 1959. On the postcranial skeleton and the outward appearance of *Spirocerus kiakhtensis* M. Pavlova. Vert PalAsiat, 3(1): 23–33

Sokolov V E, Lushchekina A A, 1997. *Procapra gutturosa*. Mamm Spec, 571: 1–5

Tedford R H, Flynn L J, Qiu Z X et al., 1991. Yushe Basin, China: paleomagnetically calibrated mammalian biostratigraphic

standard for the Late Neogene of eastern Asia. J Vert Paleontol, 11(4): 519–526

Teilhard de Chardin P, Leroy P, 1942. Chinese fossil mammals: a complete bibliography, analyzed, tabulated, annotated and indexed. Inst Geo-Biol Pék, 8: 1–142

Teilhard de Chardin P, Piveteau J, 1930. Les mammifères fossiles de Nihowan (Chine). Ann Paléontol, 19: 1–134

Teilhard de Chardin P, Trassaert M, 1938. Cavicornia of south-eastern Shansi. Palaeontol Sin New Ser C, 6: 1–98

Teilhard de Chardin P, Young C C, 1936. On the mammalian remains from the archaeological site of Anyang. Palaeontol Sin Ser C, 1: 1–61

Tong H W, 2012. New remains of *Mammuthus trogontherii* from the Early Pleistocene Nihewan beds at Shanshenmiaozui, Hebei. Quat Int, 255: 217–230

Tong H W, Chen X, 2016. On newborn calf skulls of Early Pleistocene *Mammuthus trogontherii* from Shanshenmiaozui in Nihewan Basin, China. Quat Int, 406: 57–69

Tong H W, Wang X M, 2014. Juvenile skulls and other postcranial bones of *Coelodonta nihowanensis* from Shanshenmiaozui, Nihewan Basin, China. J Vert Paleontol, 34(3): 710–724

Tong H W, Zhang B, 2019. New fossils of *Eucladoceros boulei* (Artiodactyla, Mammalia) from Early Pleistocene Nihewan Beds, China. Palaeoworld, 28(3): 403–424

Tong H W, Hu N, Han F, 2011. A preliminary report on the excavations at the Early Pleistocene fossil site of Shanshenmiaozui in Nihewan Basin, Hebei, China. Quat Sci, 31: 643–653

Tong H W, Hu N, Wang X M, 2012. New remains of *Canis chihliensis* (Mammalia, Carnivora) from Shanshenmiaozui, a Lower Pleistocene Site in Yangyuan, Hebei. Vert PalAsiat, 50(4): 335–360

Tong H W, Wang F G, Zheng M et al., 2014. New fossils of *Stephanorhinus kirchbergensis* and *Elasmotherium peii* from the Nihewan Basin. Acta Anthropol Sin, 33(3): 369–388

Tong H W, Chen X, Zhang B, 2017. New fossils of *Bison palaeosinensis* (Artiodactyla, Mammalia) from the steppe mammoth site of Early Pleistocene in Nihewan Basin, China. Quat Int, 445: 250–268

Tong H W, Chen X, Zhang B, 2018. New postcranial bones of *Elasmotherium peii* from Shanshenmiaozui in Nihewan Basin, northern China. Quaternaire, 29 (3): 195–204

Tong H W, Zhang B, Chen X et al., 2021. Chronological significance of the mammalian fauna from the Early Pleistocene Shanshenmiaozui site in Nihewan Basin, northern China. Acta Anthropol Sin, 40(3): 469–489

Tong Y S, Zheng S H, Qiu Z D, 1995. Cenozoic mammal ages of China. Vert PalAsiat, 33(4): 290–314

Viret J, 1954. Le Loess à bancs durcis de Saint-Vallier (Drôme) et sa faune de mammifères villafranchiens. Nouv Arch Mus Hist Nat Lyon, 4: 1–200

Vislobokova I A, 2008. The major stages in the evolution of Artiodactyl communities from the Pliocene–Early Middle Pleistocene of northern Eurasia. Paleontol J, 42(3): 297–312; 42(4): 414–424

Vislobokova I, Dmitrieva E, Kalmykov N, 1995. Artiodactyls from the Late Pliocene of Udunga, western trans-Baikal, Russia. J Vert Paleontol, 15: 146–159

Vislobokova I A, Titov V V, 2020. Spiral-horned antelopes of the Early Pleistocene Tamanian faunal complex of eastern Europe. Russ J Theriol, 19(1): 37–44

Vislobokova I A, Titov V V, Lavrov A V et al., 2020. Early Pleistocene spiral-horned antelopes (Artiodactyla, Bovidae) from the Taurida Cave (Crimea, Russia). Paleontol J, 54: 81–90

Vrba E S, Schaller G, 2000. Phylogeny of Bovidae based on behavior, glands, skulls, and postcrania. In: Vrba E S, Schaller

G eds. Antelopes, Deer, and Relatives. New Haven: Yale University Press. 203–222

Wang Y R, Peters J, Barker G, 2020. Morphological and metric criteria for identifying postcranial skeletal remains of modern and archaeological Caprinae and Antilopinae in the northeast Tibetan Plateau and adjacent areas. Int J Osteoarchaeol, 30(4): 492–506

Young C C, 1932. On the Artiodactyla from the *Sinanthropus* Site at Choukoutien. Palaeontol Sin Ser C, 8(2): 1–100

Zhang Z Q, Yang R, 2016. Morphology and taxonomy of *Gazella* (Bovidae, Artiodactyla) from the Late Miocene Bahe Formation, Lantian, Shaanxi Province, China. Vert PalAsiat, 54(1): 1–20

Zhu R X, Hoffman K A, Potts R et al., 2001. Earliest presence of humans in Northeast Asia. Nature, 413: 413–417